Investigation of Shock-Induced Turbulent Mixing at a Gas Interface

Riccardo Bonazza, David Rothamer, Jason Oakley, Dan Reese

University of Wisconsin-Madison

National Nuclear Security Administration (NNSA)
2016 Stewardship Science Academic Programs(SSAP) Symposium
Bethesda, February 17-18, 2016

Background: The Richtmyer-Meshkov Instability

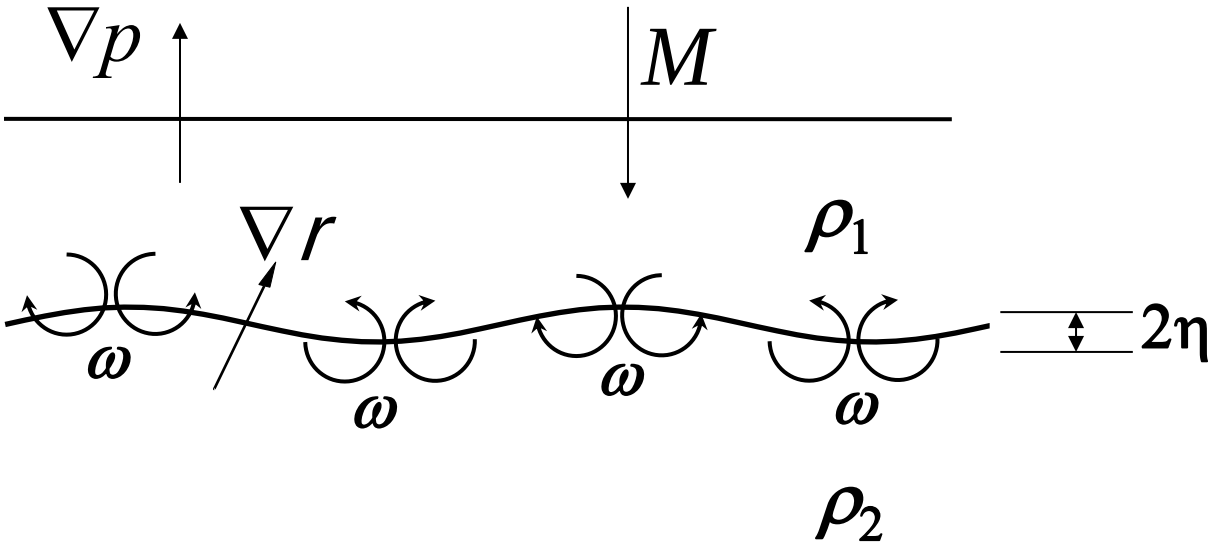

Baroclinic vorticity generation:

$$\frac{dw}{dt} = \frac{\nabla r \times \nabla p}{r^2}$$

$$A = \frac{\rho_2 - \rho_1}{\rho_2 + \rho_1}$$ **Atwood number**

Background: Motivation

RMI occurs over large ranges of length and time scales, e.g. astronomy, aerospace, inertial confinement fusion (ICF)

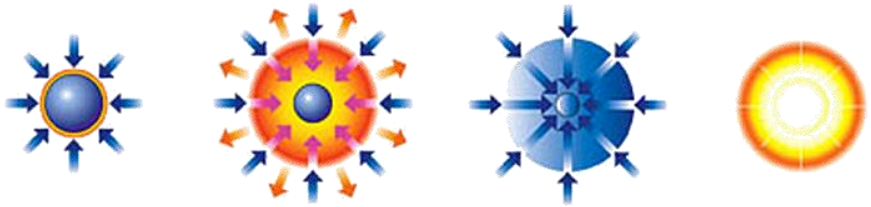

Radiative heating | Ablation | Compression | Thermo-nuclear burn

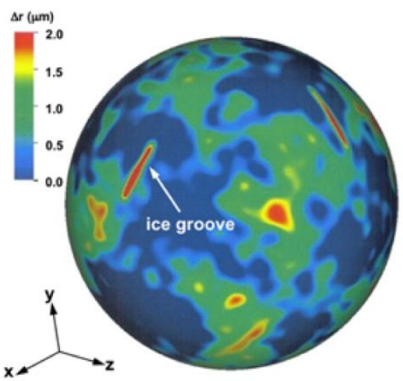

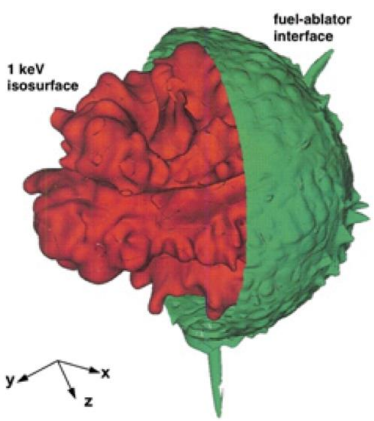

	ICF	Shock tube
L scale	10^{-6} m	10^{-2} m
t scale	10^{-9} s	10^{-6} s
ρ scale	10^{3} kg/m^3	10^{0} kg/m^3
M	~30	≤ 5
A	[-1,1]	[-1,1]

Background: The Richtmyer-Meshkov Instability

Impulsive (linear) model for 2-D single mode:
R. Richtmyer, 1960

$$h = k[V]Ah_0 t$$

- k: wavenumber
- $[V]$: velocity jump
- $A = \frac{\rho_2 - \rho_1}{\rho_2 + \rho_1}$

Valid for $\eta << \lambda$

First experiments: E. Meshkov, 1969

Broader view

More representative initial conditions

- **Multimode**
- **Three-dimensional**

Challenges

- **Linear superposition only if $\eta << \lambda$ for ALL λs**
- **$\eta \sim \lambda$ very quickly for high wavenumbers**
- **Departure from linear growth**
- **Saturation**

Open questions

- **Evolution of macroscopic properties ($h=h(t)$)**
- **Characteristic lengths (λ_T , λ_B , η)**
- **Mixing rates**
- **Scaling laws** $\left(e.g. \frac{h(t)}{h_0'} = a \left(\frac{\dot{h}_0}{h_0'} t \right)^{\theta} \right)$
- **Dependence upon: I.C., *A*, *M***

Approach

- **Measure 2-D fields (concentration, velocity)**
- **Extract integral quantities (*e.g. h*)**
- **Study statistics (PDF, spectra)**
- **Extract characteristic lengths**
- **Extract vorticity field**

Experimental Setup: The WiSTL Facility

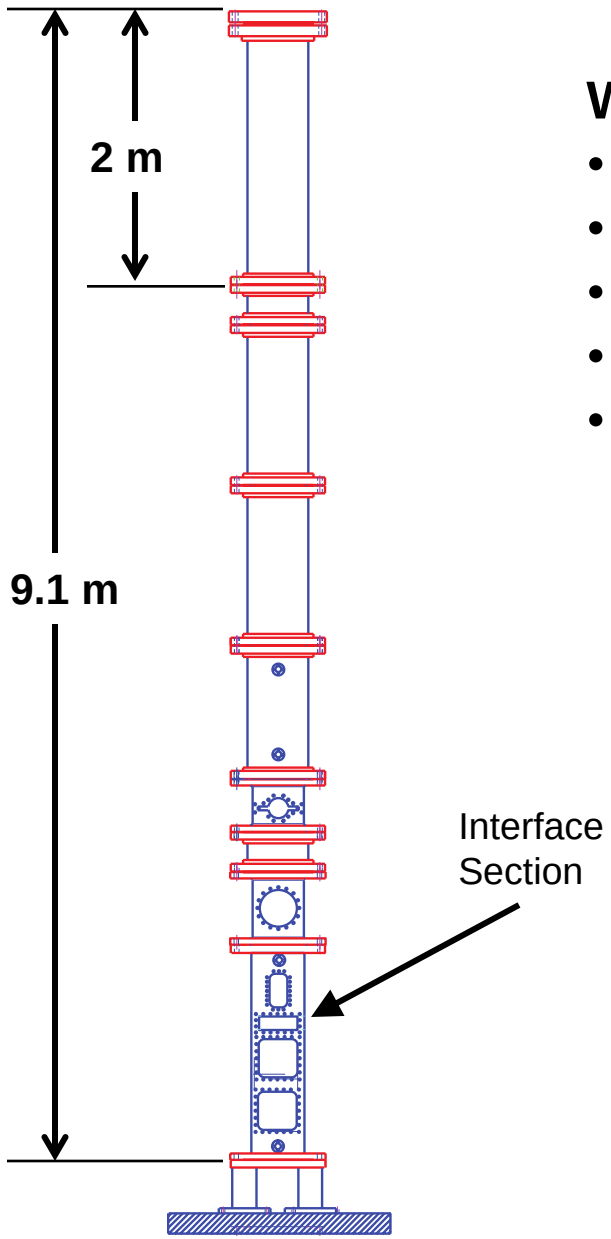

Wisconsin Shock Tube Laboratory

- Vertical
- Large internal cross-section (25 cm square)
- Total length 9.13 m, driver length 2 m
- Pressure load capability: 20 MPa
- Modular driven section

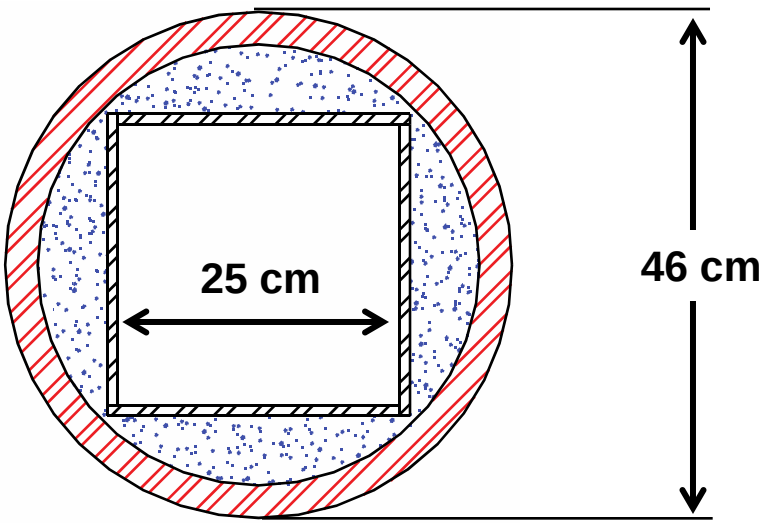

Experimental Setup: Initial Condition

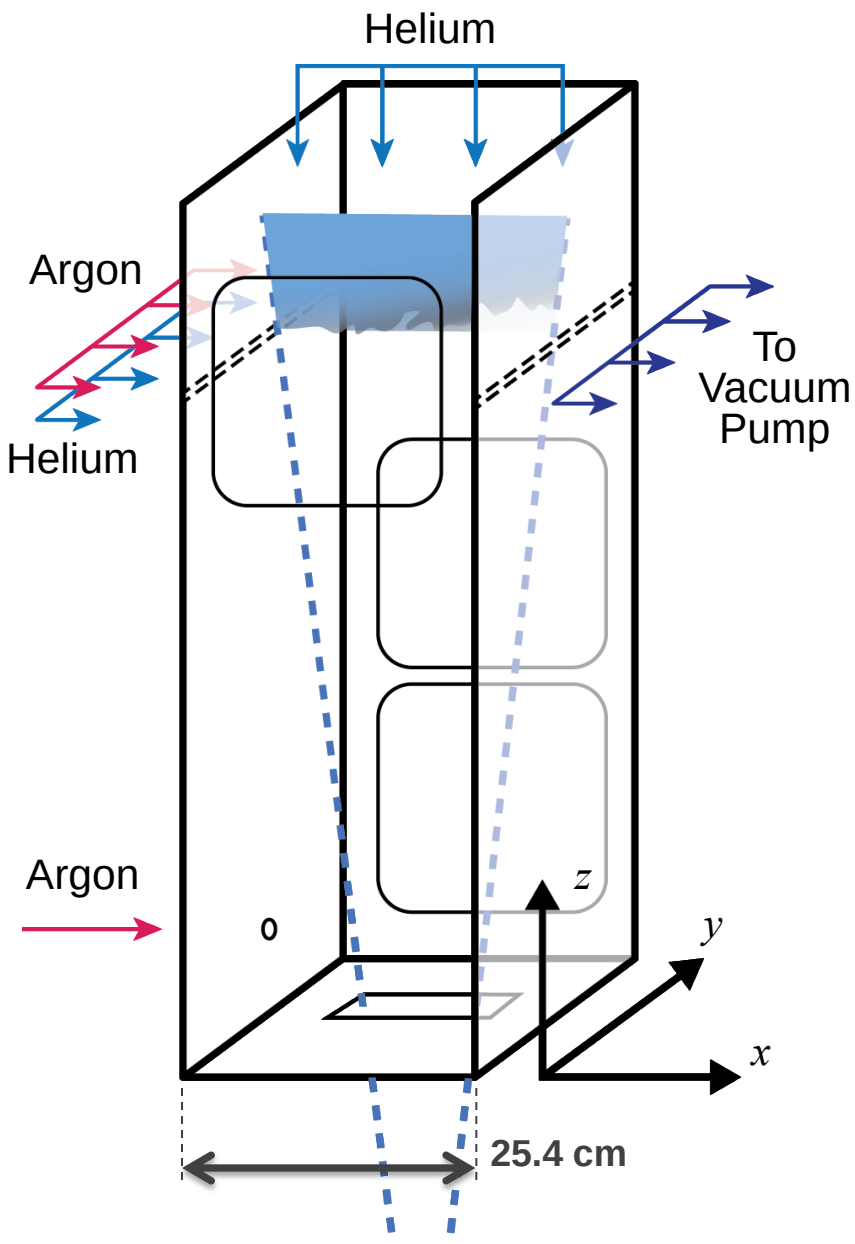

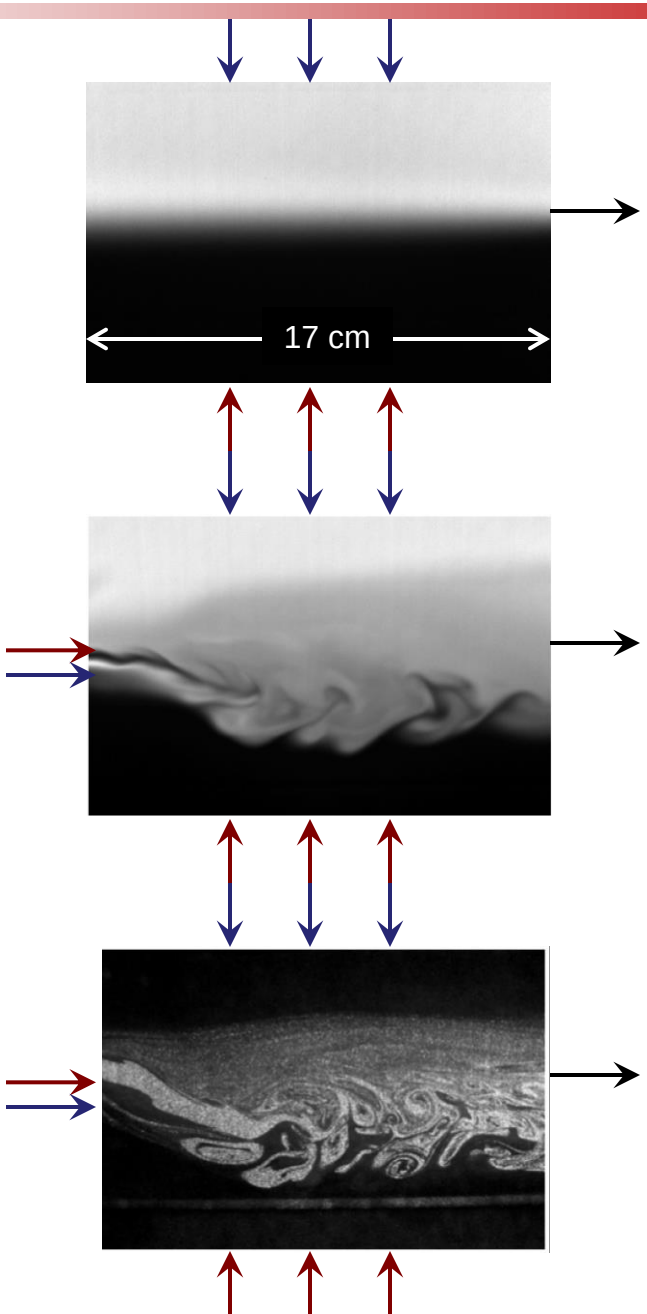

Experimental Setup: PLIF Experimental Configuration

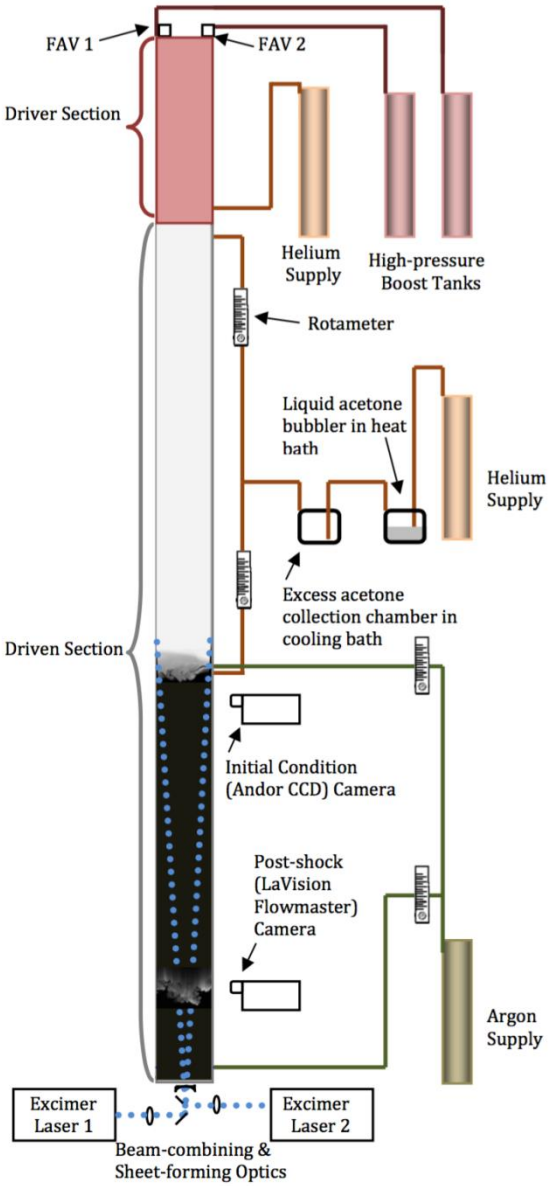

Molecular (acetone) seeding of light gas (helium)

Illumination from 308 nm excimer laser sheet

Images at 4 post-shock times

2-D concentration field

2-D mole fraction field: *M* = 2.2, *A*=0.7

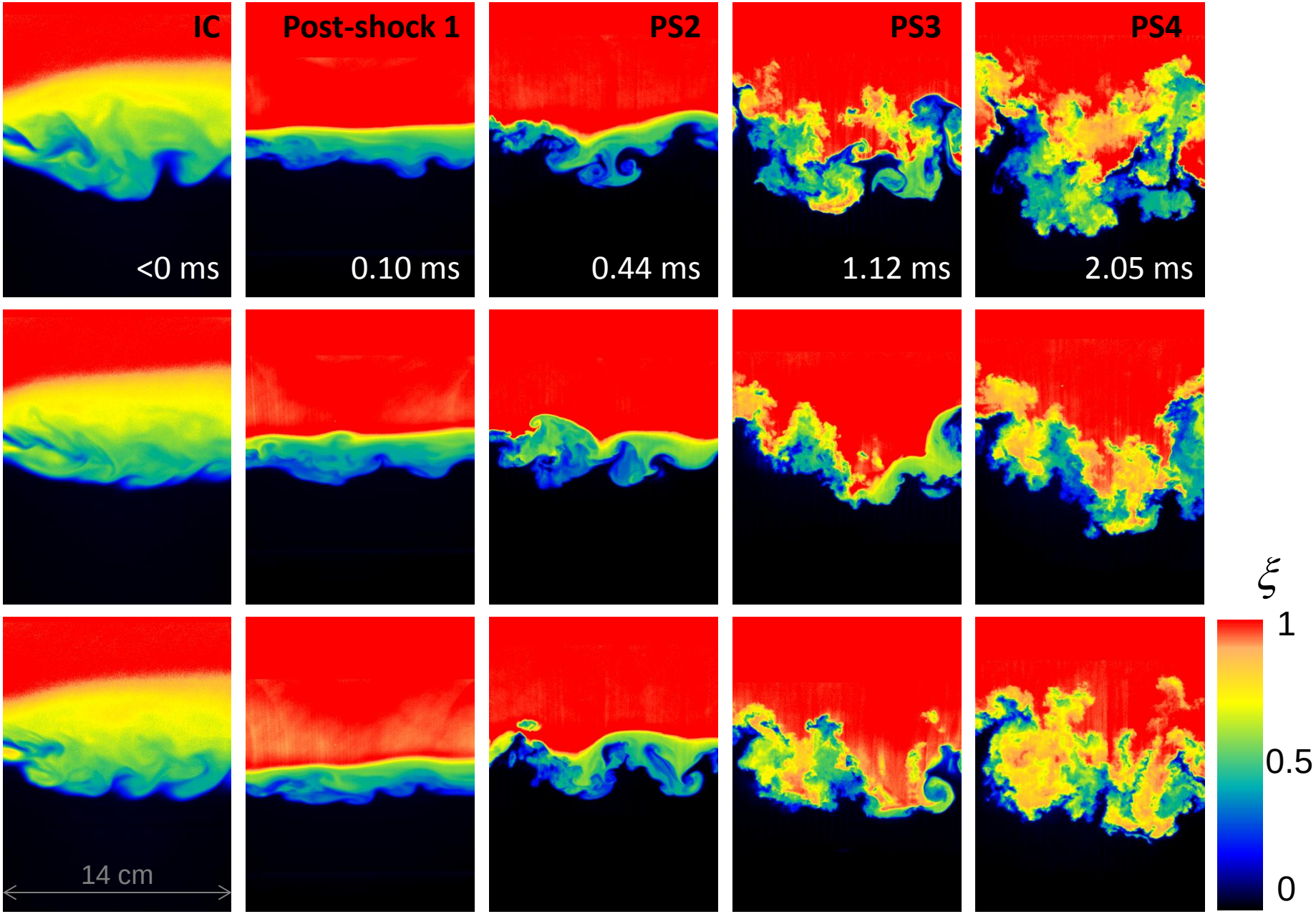

Results: Concentration—Taylor Microscale, @PS4

λ_T: length scale below which viscosity significantly affects flow
Estimated using either of two methods:

Autocorrelation Method

$$R(r) = \frac{\langle \xi^*(x)\xi^*(x+r)\rangle}{\langle (\xi^*)^2\rangle}$$

$$\lambda_T = \left[-\frac{1}{2}\frac{d^2R(0)}{dr^2}\right]^{-1/2}$$

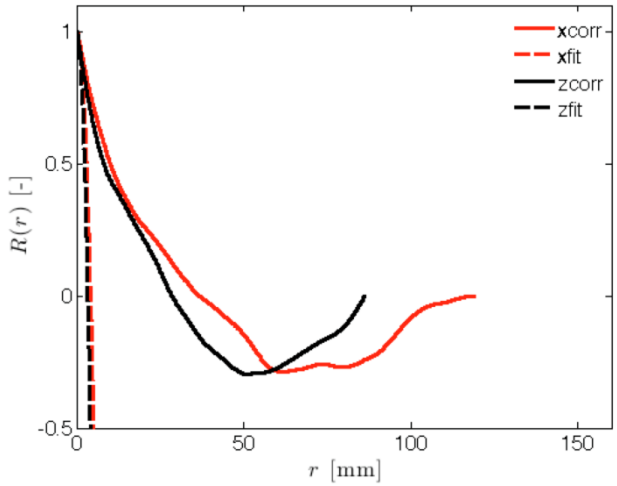

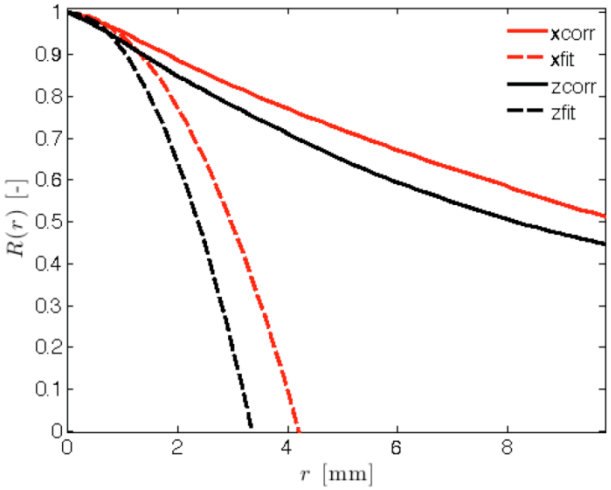

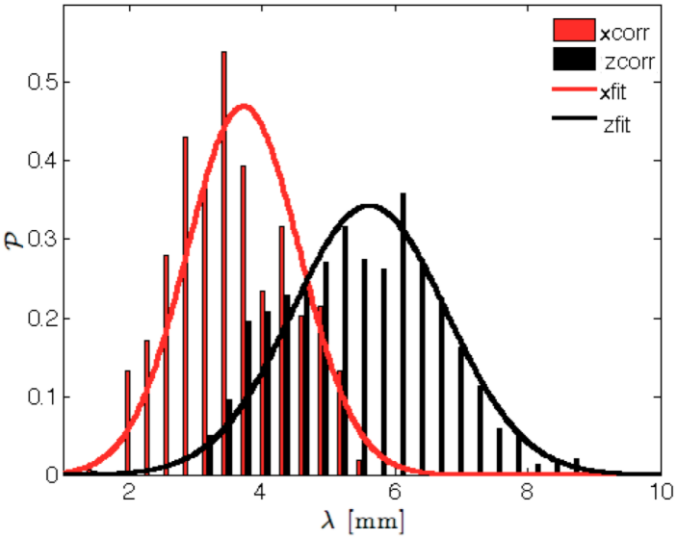

Variance Method

$$\lambda_{T,x}^2 = \frac{2\left\langle (\xi^*)^2\right\rangle}{\left\langle \left(\frac{\partial \xi^*}{\partial x}\right)^2\right\rangle}, \quad \lambda_{T,z}^2 = \frac{2\left\langle (\xi^*)^2\right\rangle}{\left\langle \left(\frac{\partial \xi^*}{\partial z}\right)^2\right\rangle}$$

$3.5\ \text{mm} < \lambda_T < 5.1$ mm
$\langle \lambda_T \rangle = 4.1$ mm

Experimental Setup: PIV Experimental Configuration

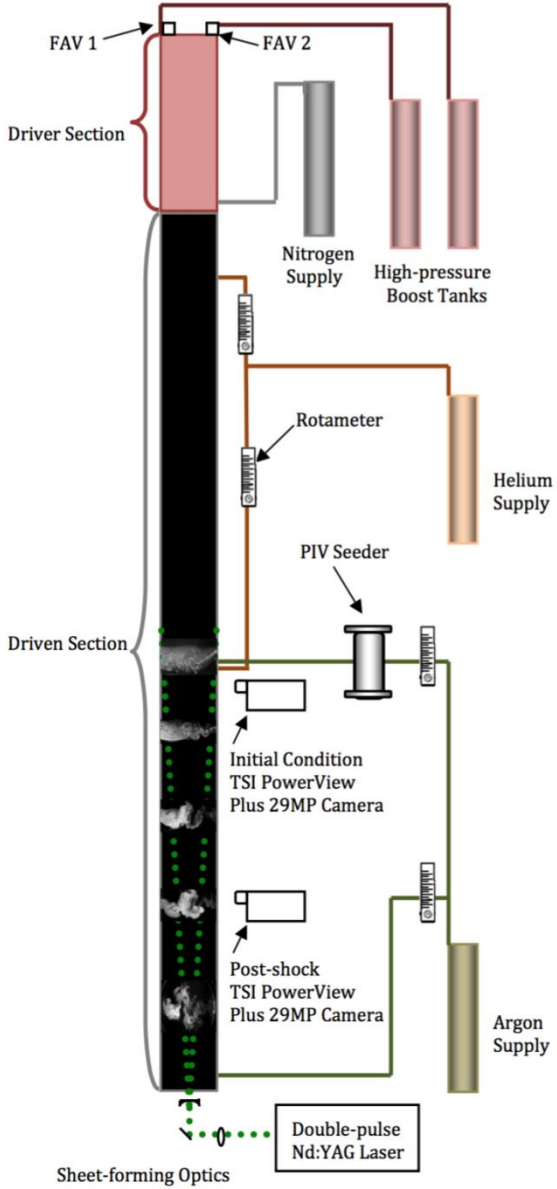

Particulate (TiO_2 diameter ~300 nm) seeding of heavy gas (argon) injection branch

Two successive particle images at 4 post-shock times

Illumination from dual-head, 532 nm Nd:YAG laser

2-D velocity field

PIV image pairs: *M* = 1.4, *A*=0.7

Post-Shock Particle Image Pairs (Δt=4 μs)

IC
(20 experiments)
t = 0 ms

PS1
(20 experiments)
t = 0.14 ms

PS2
(20 experiments)
t = 0.88 ms

PS3
(20 experiments)
t = 2.16 ms

PS4
(20 experiments)
t = 3.84 ms

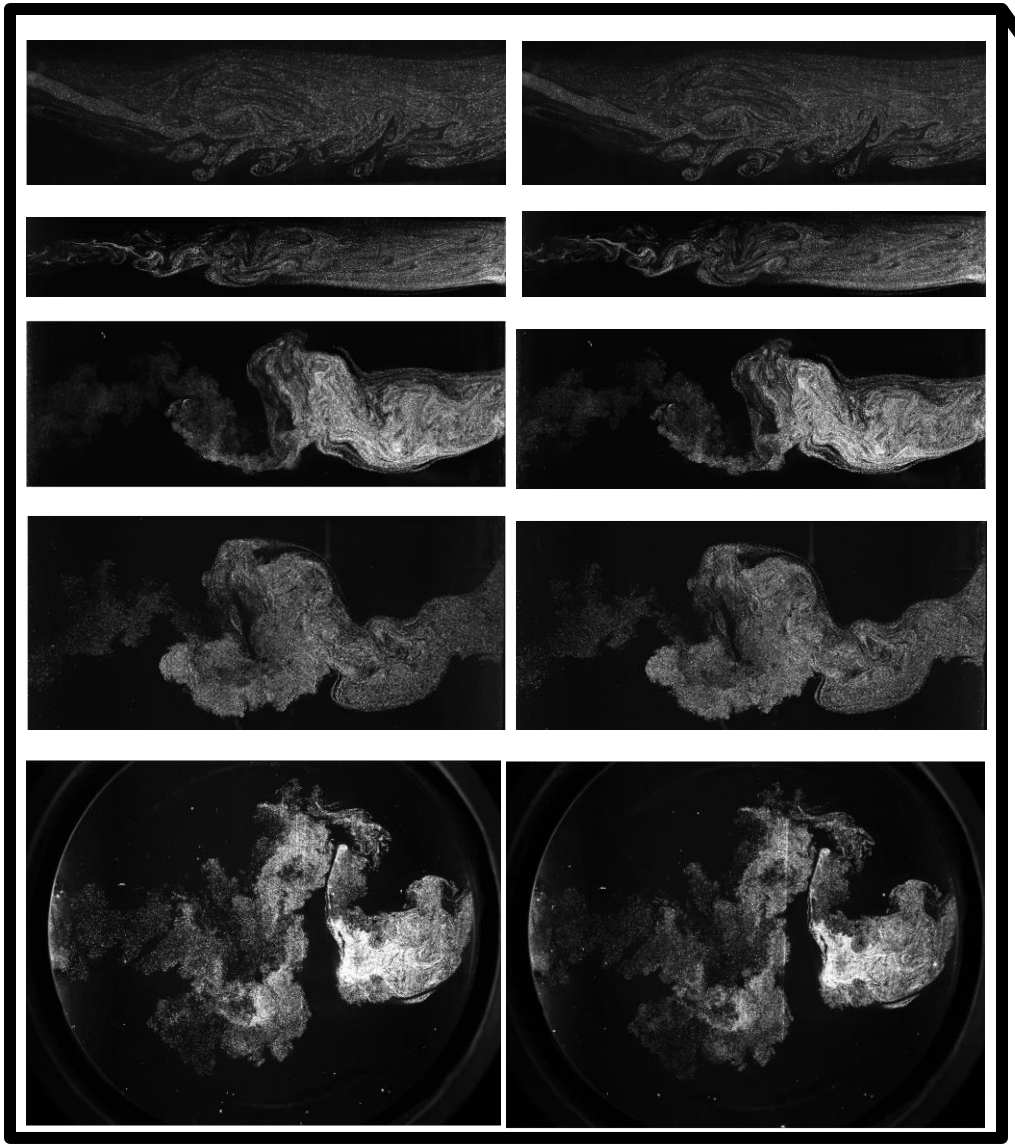

Preprocessing

Background subtraction & intensity normalization prior to performing velocimetry

Insight 4G

Proprietary particle image velocimetry (PIV) software from TSI used to extract velocity fields.

Results: Velocity Fluctuation Fields

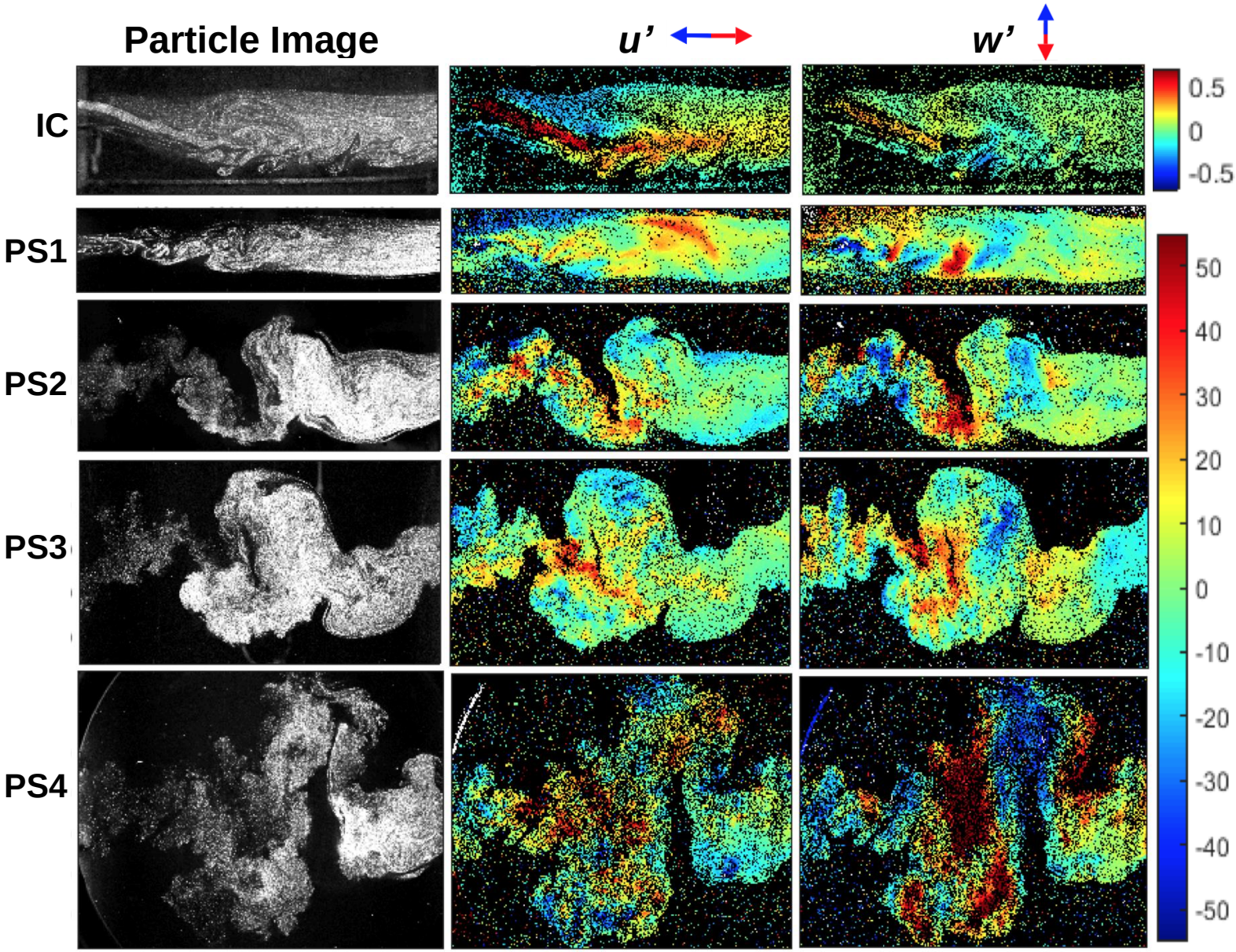

Note:

Mean velocity is subtracted from each field to give velocity fluctuations

Post-shock velocity fluctuations ~2 orders magnitude larger than IC velocities

Results: Distribution of Velocity Fluctuations

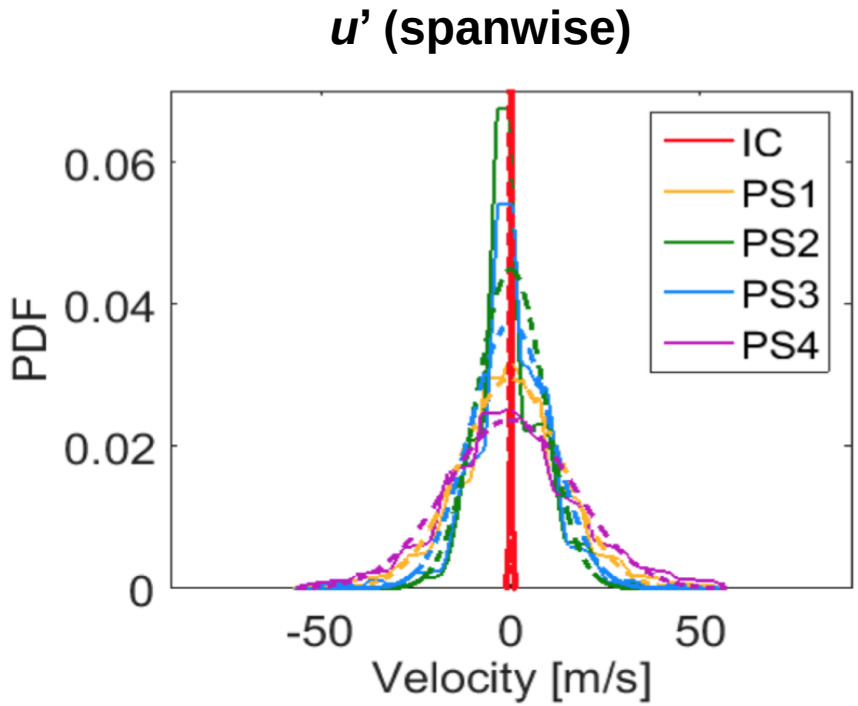

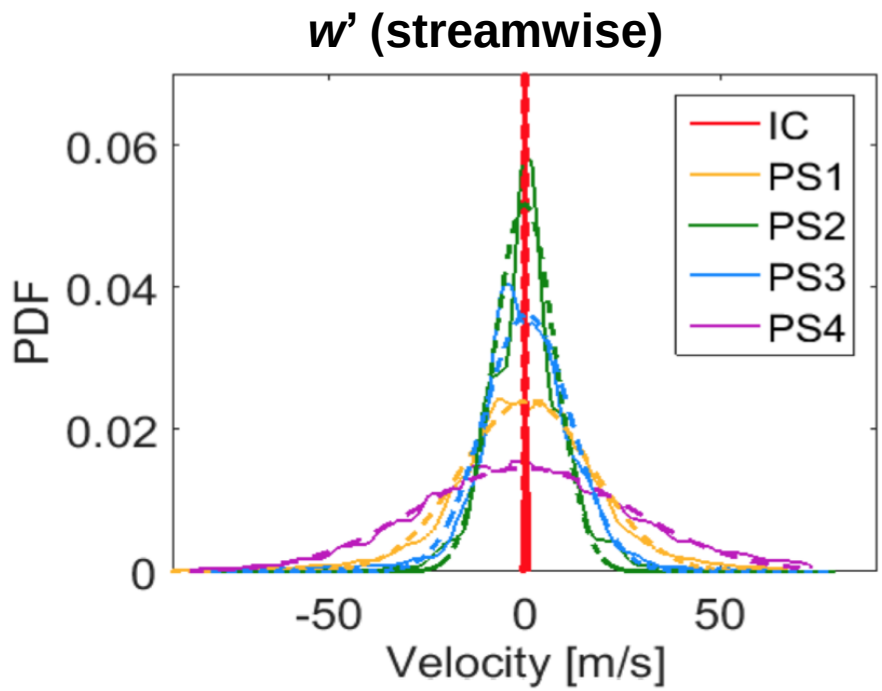

Note: Broader distribution of velocity in *z*-direction, similar to LANL gas curtain experiments (Prestridge, 2000); however, present work shows larger spread in fluctuating velocities in both directions

	u'_{RMS} (m/s)	w'_{RMS} (m/s)
IC:	0.20	0.10
PS1:	16.74	54.34
PS2:	11.72	11.97
PS3:	13.19	15.19
PS4:	32.82	58.34

Results: Planar TKE Spectra

Note: All spectra have been normalized by peak value for comparison

Increase in energy at small scales with increasing post-shock time

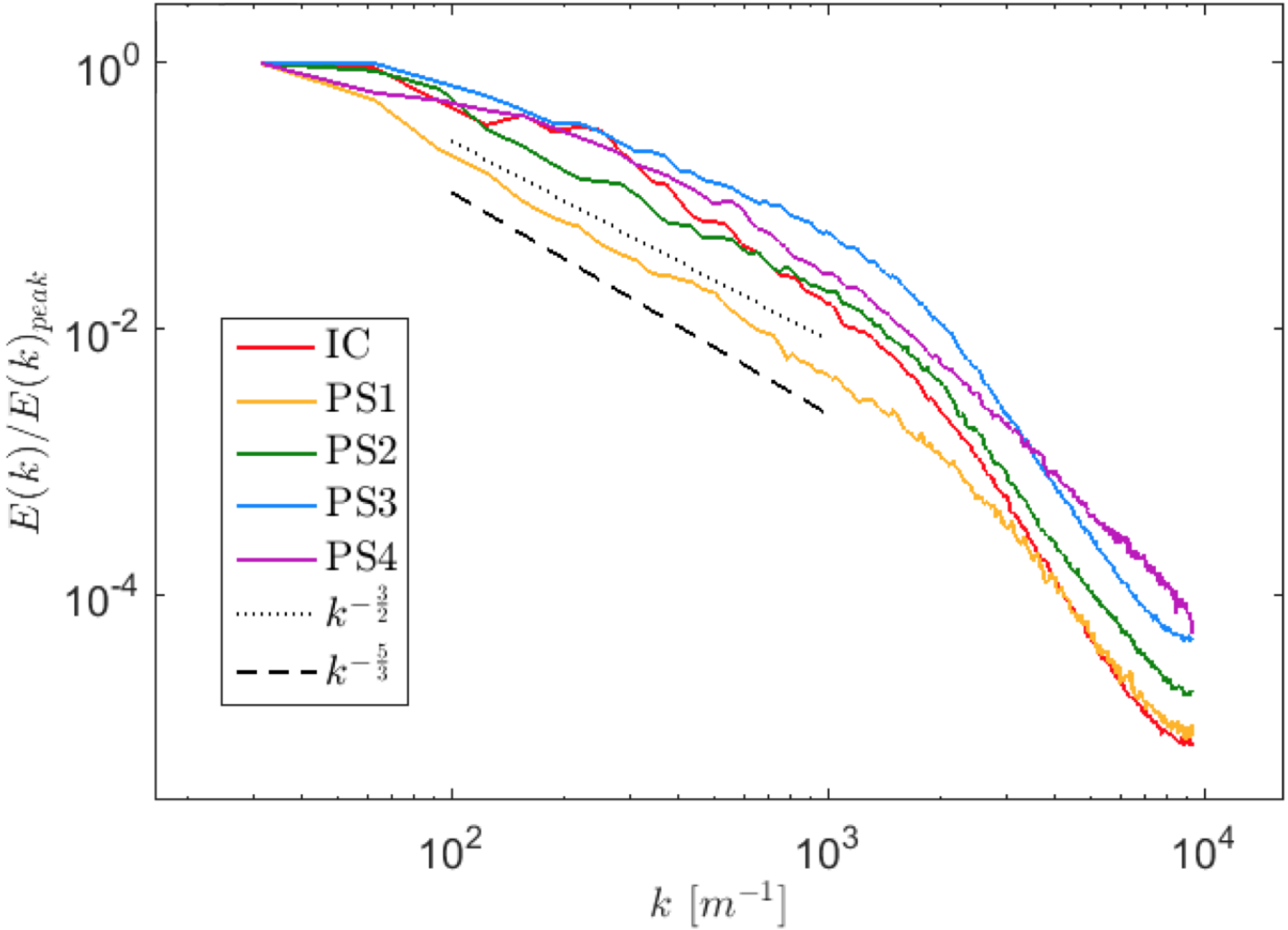

While the IC spectrum shows a rounded inertial range, there is a flattening of the spectrum for all post-shock times

Results: Higher-order statistics

Normalized velocity-derivative moments:

Velocity-derivative Skewness

$$S_{\frac{\partial u_i}{\partial x_i}} = \left[\frac{\left\langle \left(\frac{\partial u_i}{\partial x_i} \right)^3 \right\rangle}{\left\langle \left(\frac{\partial u_i}{\partial x_i} \right)^2 \right\rangle^{1.5}} \right] \text{(no sum)}$$

Velocity-derivative Kurtosis

$$K_{\frac{\partial u_i}{\partial x_i}} = \left[\frac{\left\langle \left(\frac{\partial u_i}{\partial x_i} \right)^4 \right\rangle}{\left\langle \left(\frac{\partial u_i}{\partial x_i} \right)^2 \right\rangle^{2}} \right] \text{(no sum)}$$

Measures of departure from Gaussian $(S=0\ ,\ K=3)$

Results: Higher-order statistics – *S vs. K*

Theory predicts, and previous experiments have shown (Van Atta and Antonia, 1980): $-S \sim K^{0.375}$

In present experiments: similar trend in *x*-direction,
steeper power law in *z*-direction

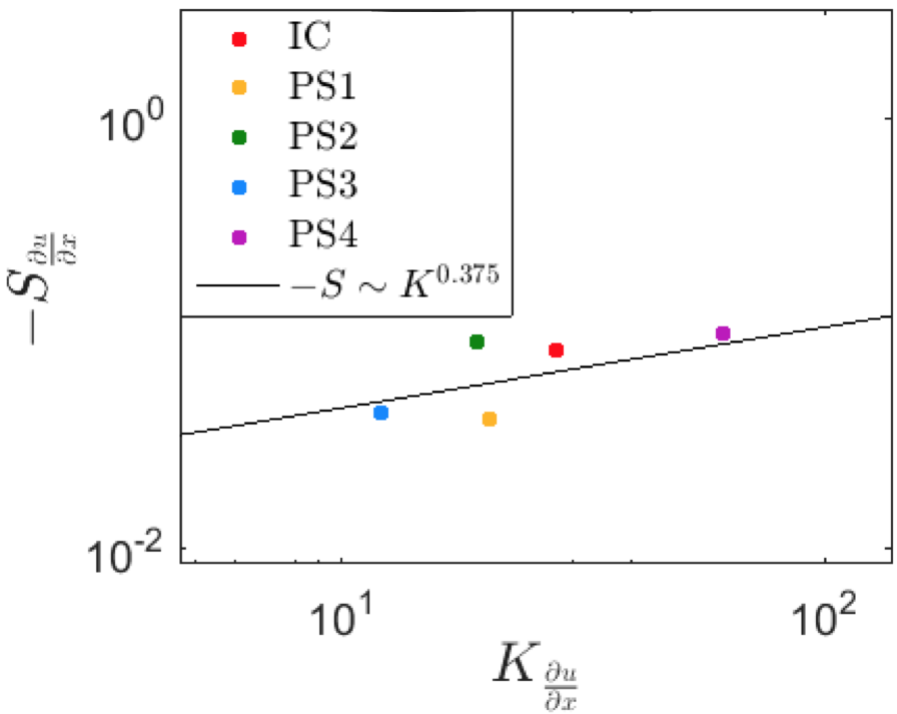

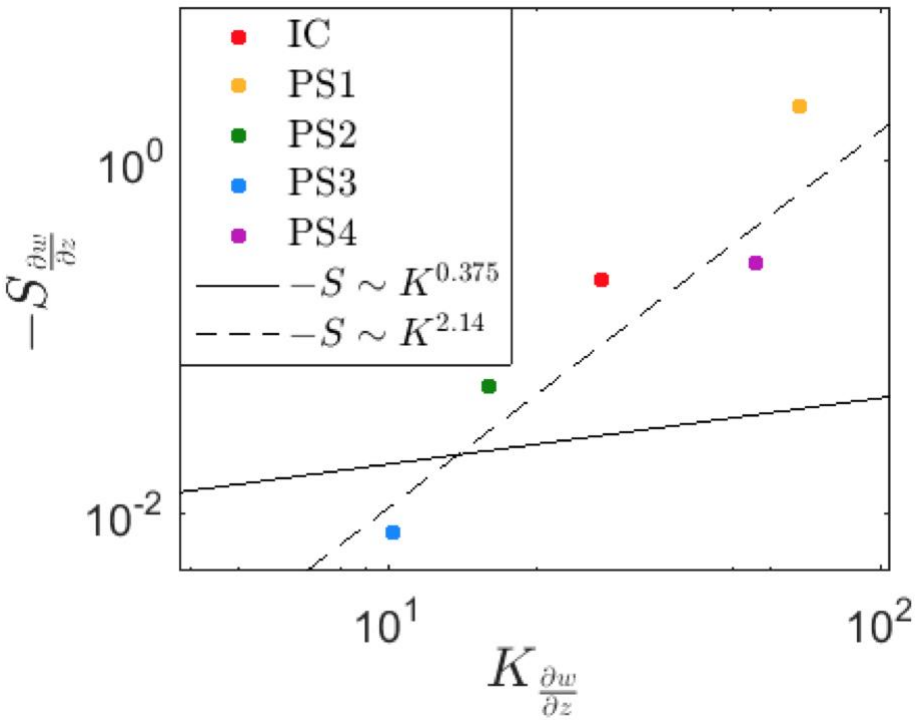

Confirms the flow anisotropy seen in the velocity-fluctuation distribution

Ideas

With **simultaneous concentration and velocity** field measurements **(not yet done)**, can:

extract Taylor microscale and RMS velocity and determine the Taylor Reynolds number:

$$Re_{\lambda,i} = \frac{\langle u_i^2 \rangle^{\frac{1}{2}} \lambda_T}{\nu}$$

If $Re_{\lambda,i} > Re_{cr}$, can calculate outer-scale Reynolds number:

$$Re = \frac{3}{20} Re_\lambda^2$$

From Re and λ_T can calculate Batchelor scale:

$$Re \simeq \frac{1}{28} \left(\frac{\lambda_T}{\lambda_B} \right)^4$$

Can calculate directional dissipation rate:

$$\epsilon_i = \frac{15\nu}{Re} \left\langle \left(\frac{\partial u_i}{\partial x_i} \right)^2 \right\rangle \quad \text{(no sum)}$$

estimate Kolmogorov scale:

$$\eta_i = \left[\frac{(\nu/Re)^3}{\epsilon_i} \right]^{\frac{1}{4}}$$

Ideas cont'd

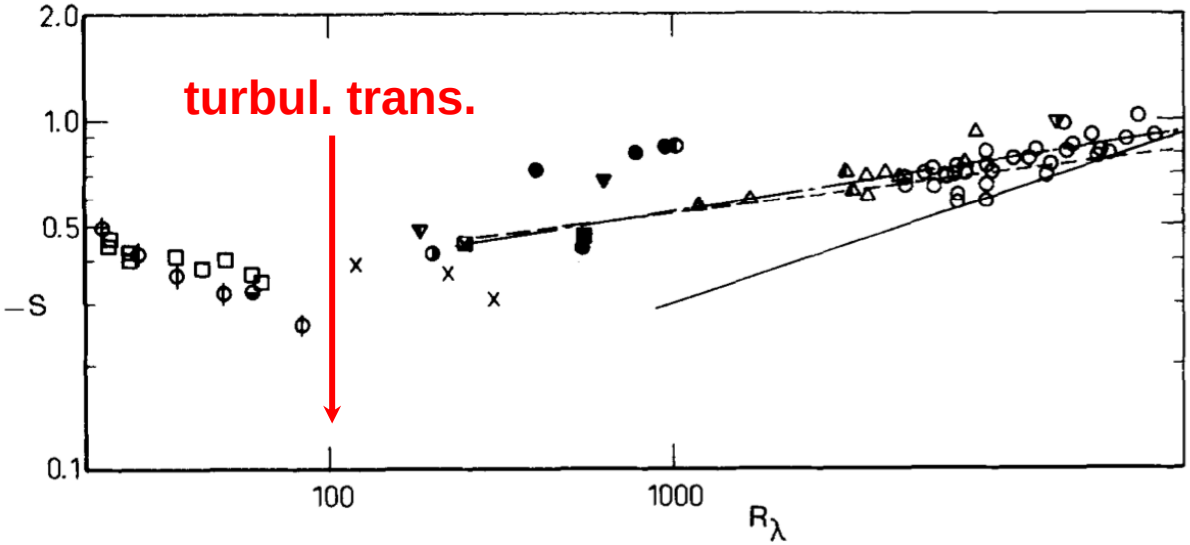

Determine $S=S(Re_\lambda)$ and

compare to $S\sim Re_\lambda^{0.13}$

(Van Atta and Antonia, 1980)

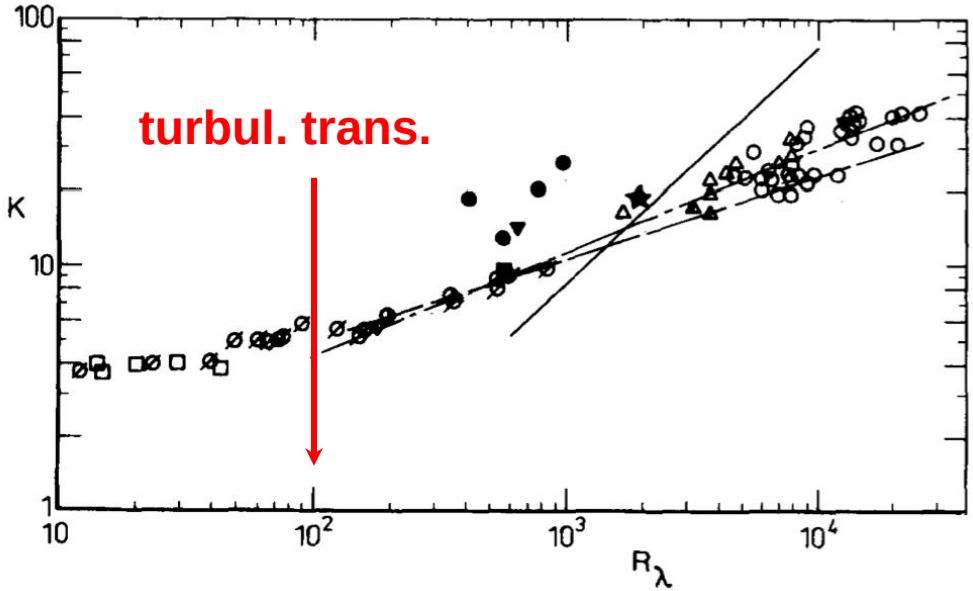

Determine $K=K(Re_\lambda)$ and

compare to $K\sim Re_\lambda^{0.35}$

(Van Atta and Antonia, 1980)

Future Work

Simultaneous PIV/PLIF measurements at IC & four post-shock times

- Molecular seeding of light gas, allowing for concentration measurements (requiring 266 nm laser sheet);
- Particulate seeding of all gas (using second PIV seeder), allowing for full-field velocity measurements (requiring 532 nm laser sheet);
- Modified laser optical setup will allow for copropagation of 266 nm and 532 nm laser light;

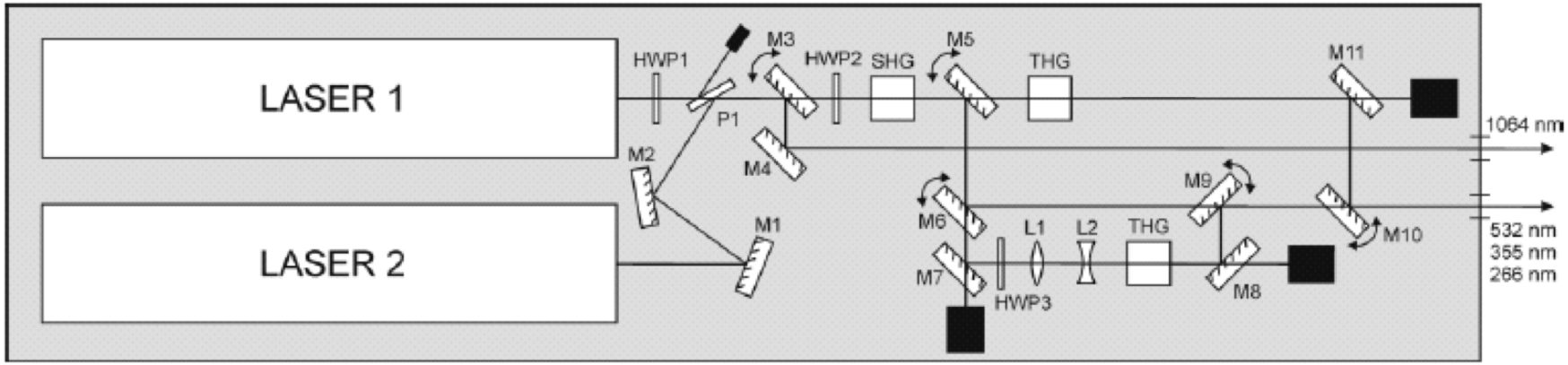

Questions?

Extra Slides

PLIF movie: Nikon 36.3 MP @ 60 fps, excimer laser @308 nm up to 100 Hz

Andor CCD (1MP) spatial resolution: 144 μm

TSI CCD (29 MP) spatial resolution: 45 μm

TiO_2 particle size: 300 nm

Post-shock interface velocity, *M*=1.4: *w*=270 m/s

Post-shock interface velocity, *M*=2.2: *w*=605 m/s

Post-shock temperature in Ar, *M*=1.4: *T*=500 K

Post-shock temperature in Ar, *M*=2.2: *T*=750 K

Taylor scale: below it, viscous effects

Batchelor scale: below it, molecular diffusion effects

Kolmogorov scale: smallest scale

Results: Vorticity Fields & Distribution

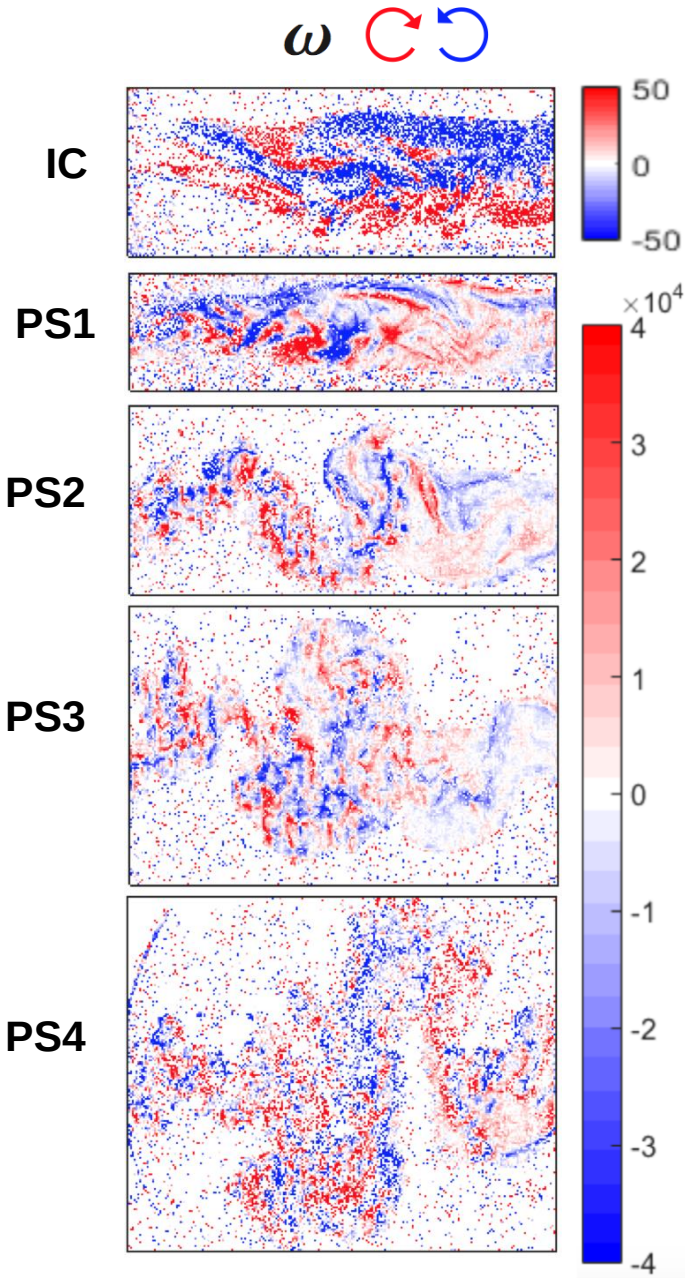

Vorticity defined by:

$$\omega \equiv \nabla \times u$$

Evolution of Vorticity Distribution

Initial peaking, followed by
a spreading at late times

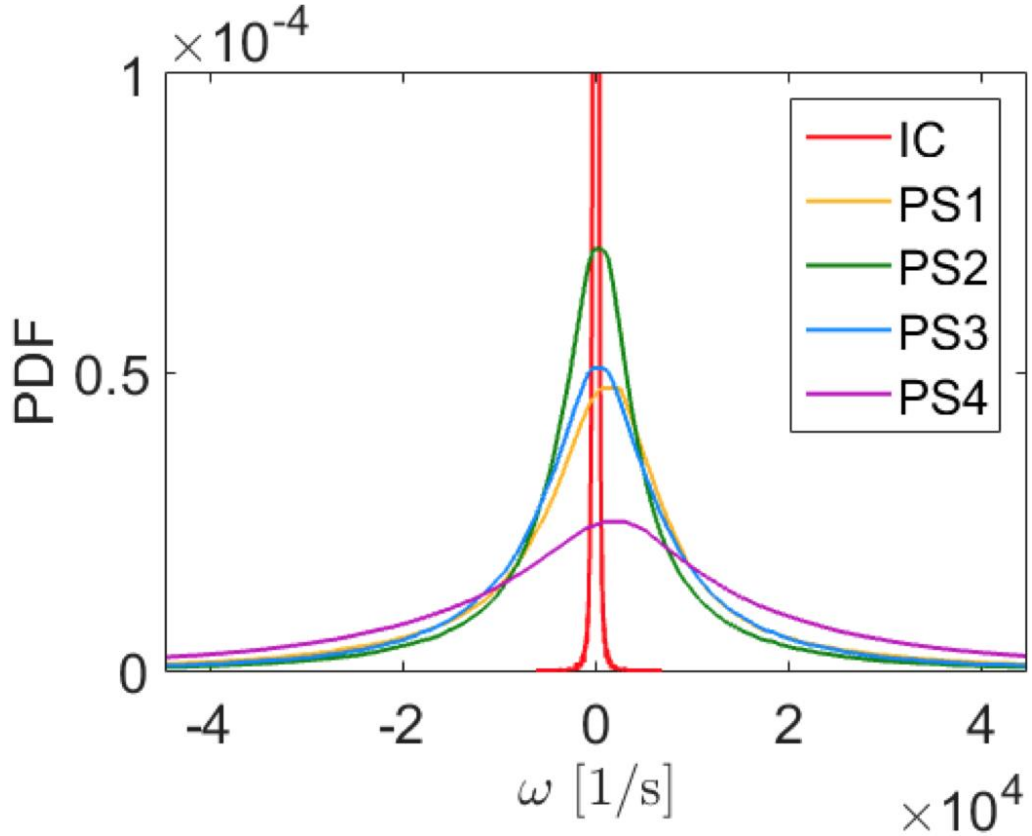

Background & Motivation

Broadband initial condition develops into a turbulent mixing zone

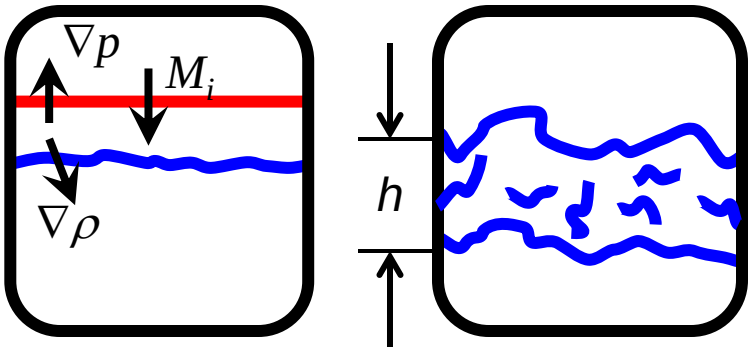

$$\frac{D\vec{\omega}}{Dt} = (\vec{\omega}\cdot\nabla)\vec{V} - \vec{\omega}\left(\nabla\cdot\vec{V}\right) + \nu\nabla^2\vec{\omega} + \frac{1}{\rho^2}(\nabla\rho\times\nabla p)$$

Current Work

- Velocity-fluctuation evolution
  - Two successive particle images to obtain velocity using PIV at 4 post-shock times.

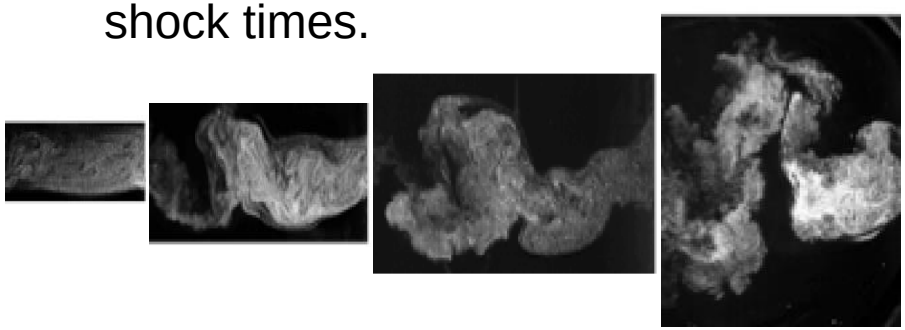

Previous Studies

- Shear layer experiments (Weber 2012)
  - Single PLIF image to obtain concentration at 4 post-shock times

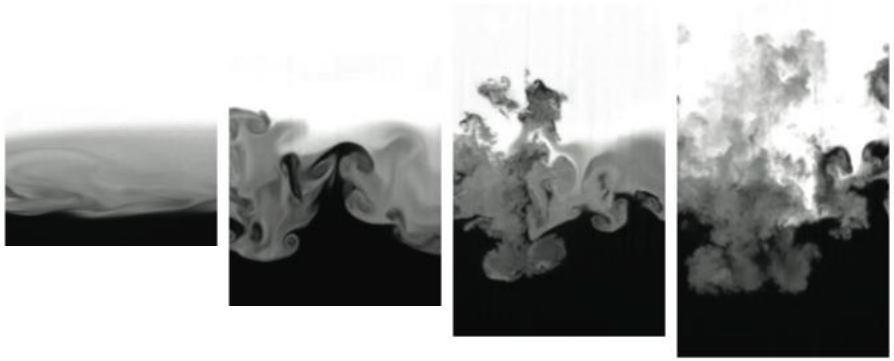

- Late-time velocity (Reese 2014)
  - Two successive PLIF images at latest time for CIV to obtain velocity

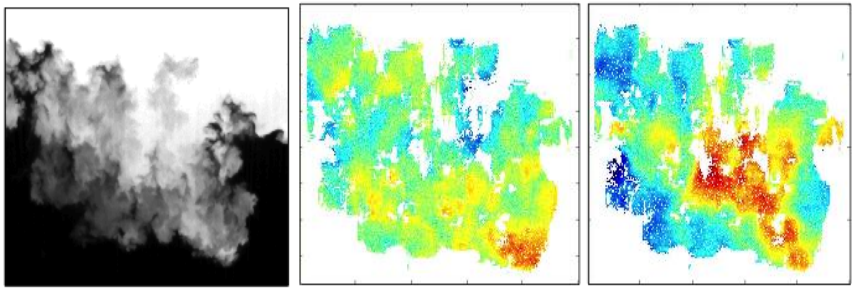

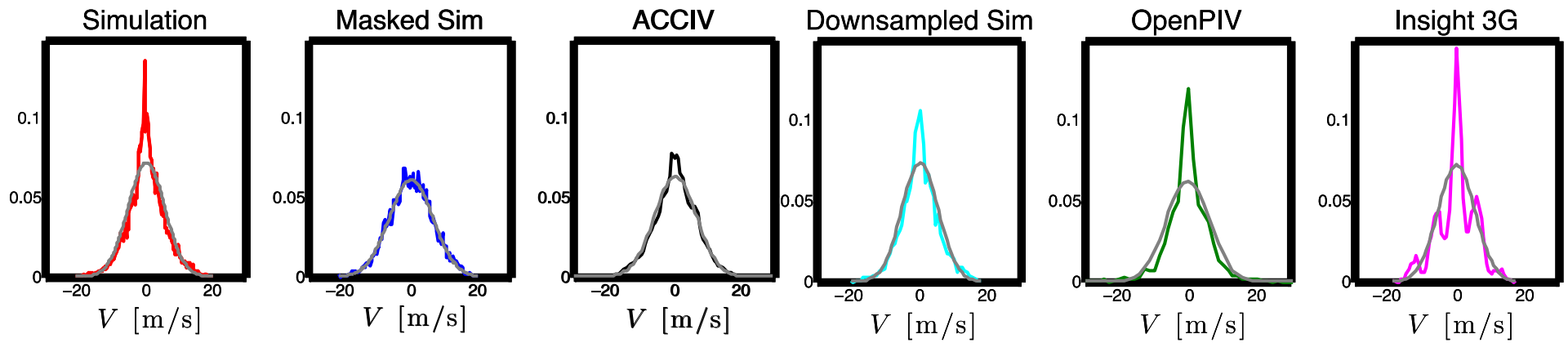

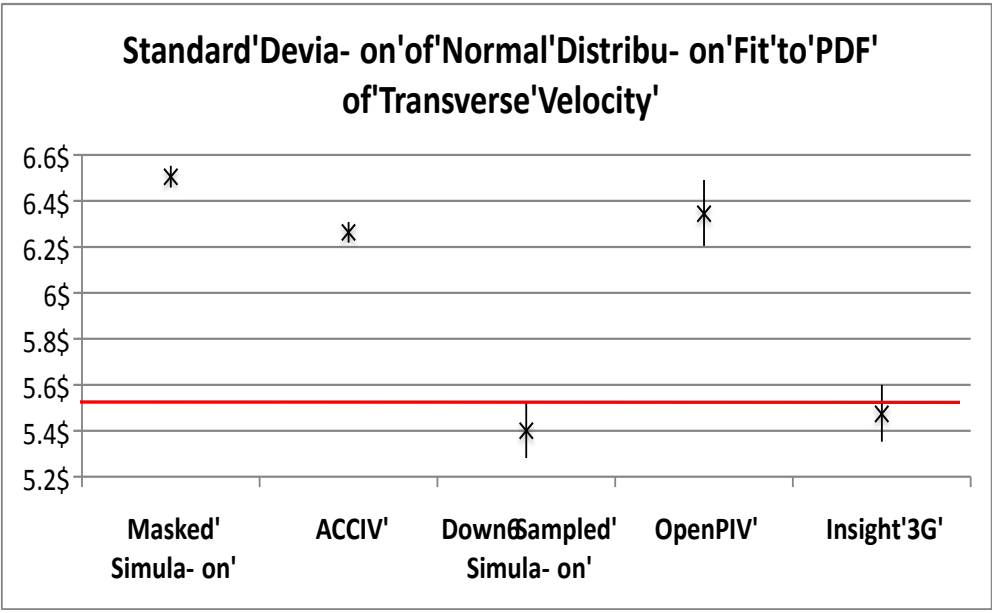

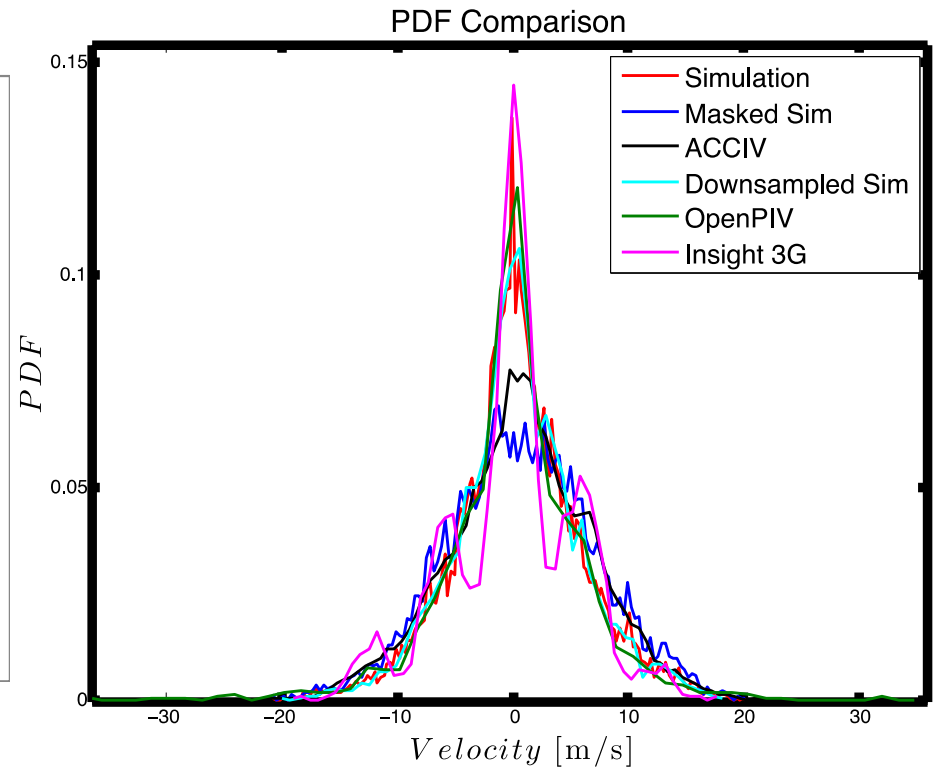

: simulation standard deviation value

Results: Concentration—Image Processing

Raw Experimental Post-Shock Image Pair

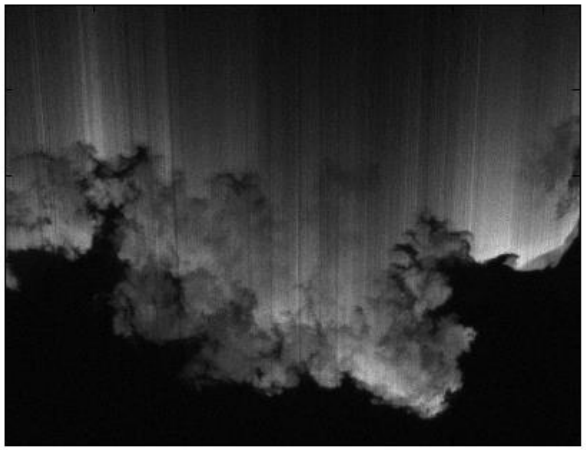

Corrected for:

- **Non-uniform laser profile**
- **Laser sheet divergence**
- **Beer's law attenuation**

Light Gas Mole Fraction

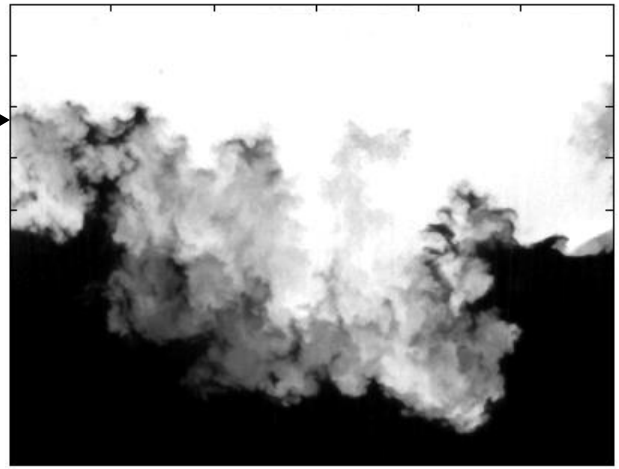

Fluorescence Signal

$$S_f = h_{opt} I n s f dV$$

Beer's Law

$$dI = - I n s \, dr$$

Number Density

$$n = C_0 x \frac{T_0}{T}$$

Compute mole fraction assuming top of image is at a constant concentration of $\xi = 1$

$$x = \frac{S_f}{S_{f,R} - C_0 s \int_r^R S_f \, dr}$$

(assuming constant temperature)

Results: Concentration

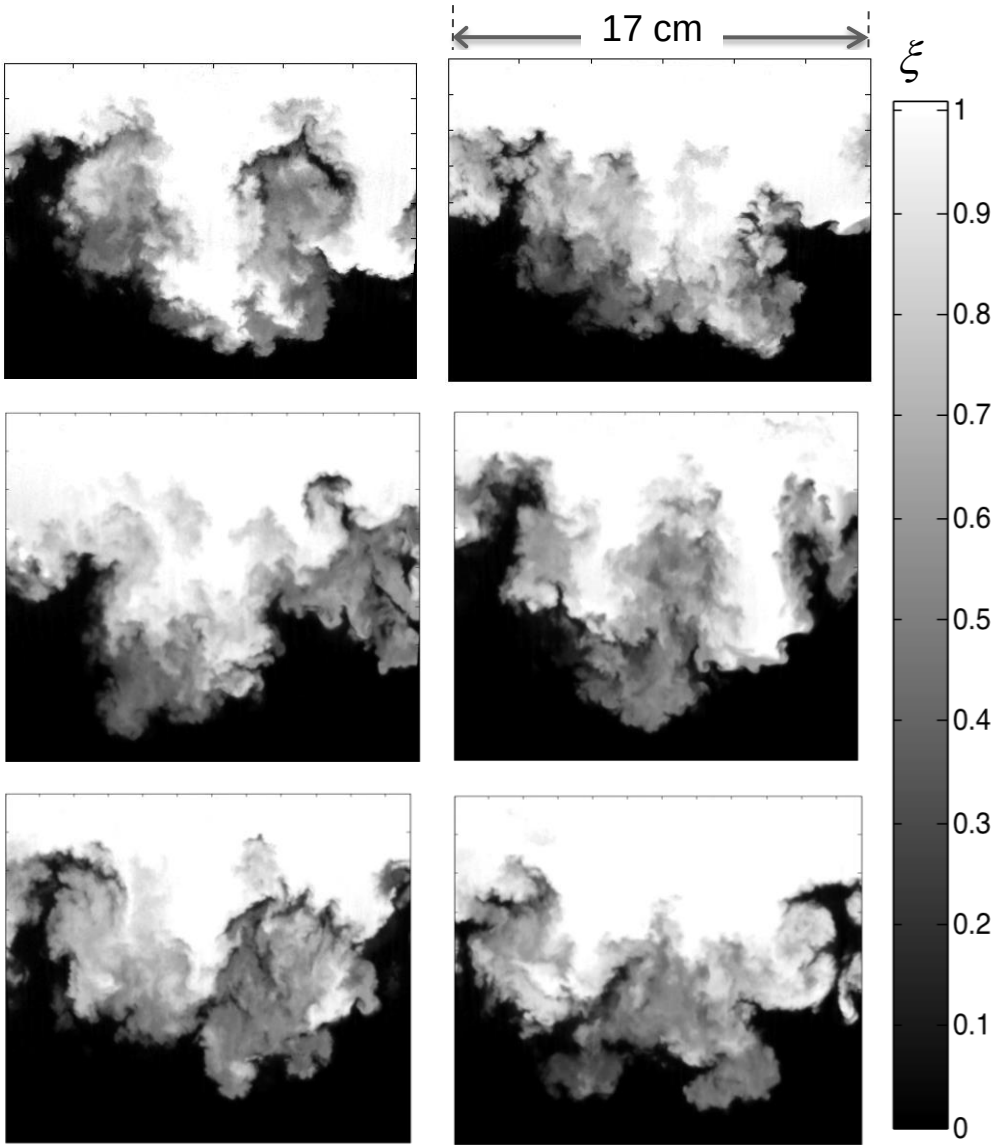

Shown: Six corrected post-shock images, all at latest (PS4) time.

20 Total

From mole fraction images:

- Scalar Variance Energy Spectrum
- Taylor Microscale

Results: Concentration—Scalar Variance Energy Spectrum

Interlacing Technique

$$E(k_x) = F(\xi_j(x))F^*(\xi_{j+1}(x)).$$

Reduces influence of noise

Spectrum shows slope $E \sim k^{-5/3}$ in inertial range, with steeper drop off at higher wave numbers

Normalized 1D Scalar Variance Energy Spectrum

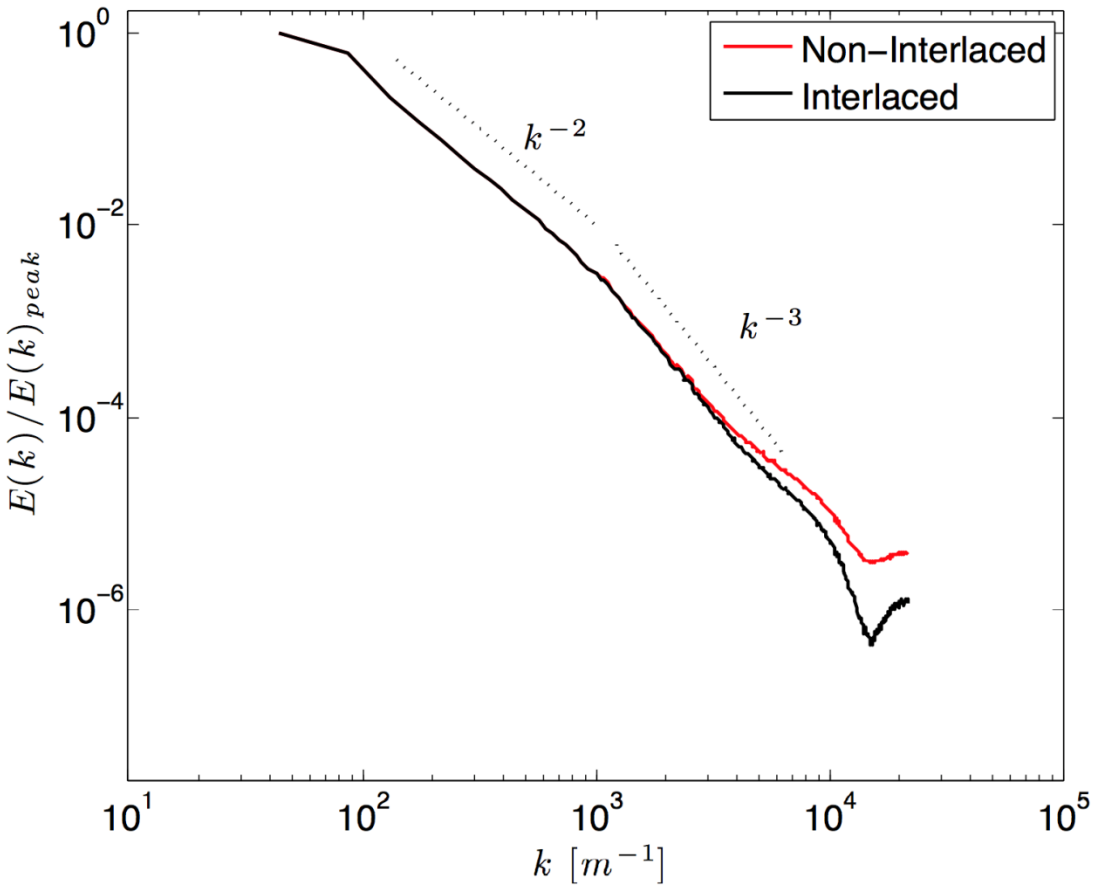

Results: Velocity—Correlation Image Velocimetry

$A = 0.7$
$M = 2.2$

Post-Shock Image Pairs (Δt=30μs)

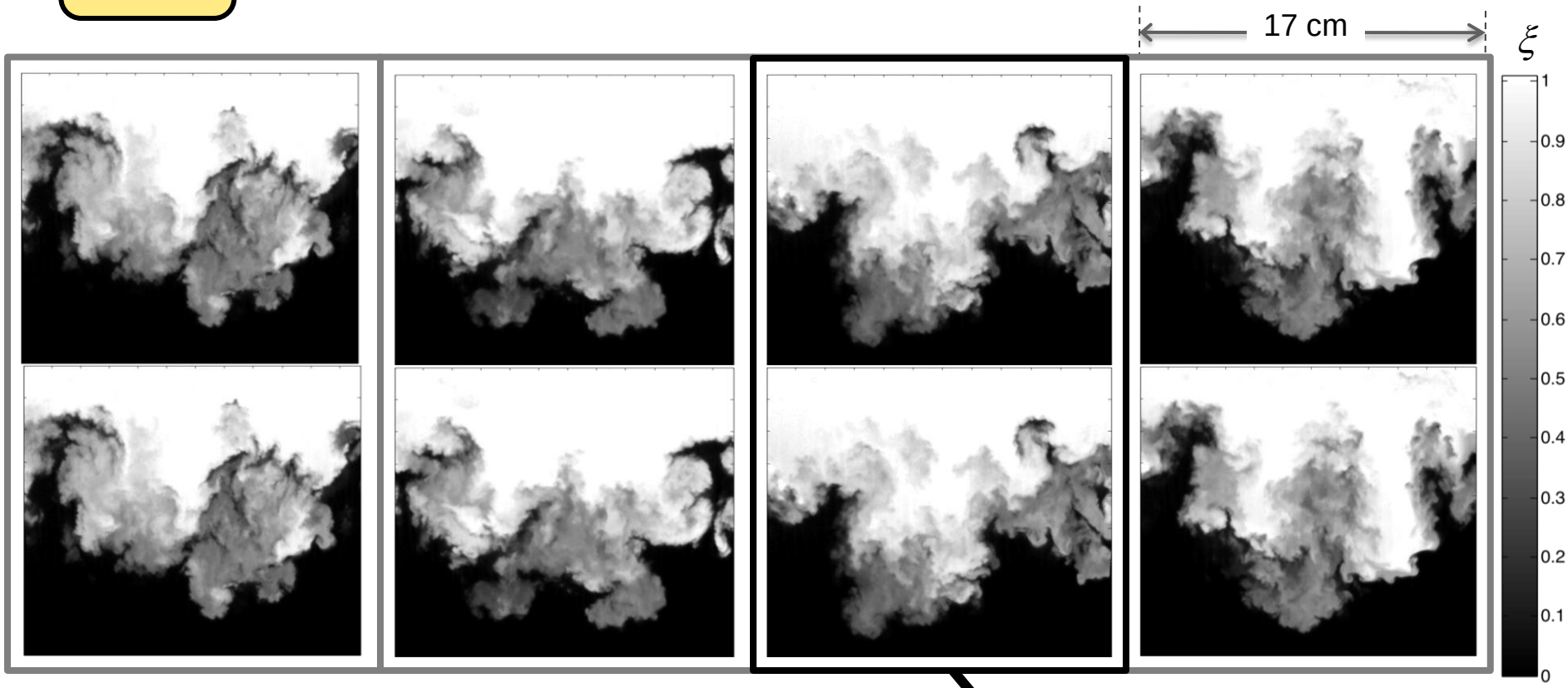

PS1
t_1 = 2.055 ms
$h_{5\text{-}95\%}$=9 cm
(20 images)

PS2
t_2 = 2.085 ms
$h_{5\text{-}95\%}$=9 cm
(20 images)

ACCIV
Particle-free velocity field extraction

Results: Numerical Validation

Can the ACCIV technique be applied to a shock−accelerated mixing layer to yield accurate results?

To answer, must perform a priori comparison against known fields.

Comparison with Simulation (Effects of masking velocity field)

- Visual comparison of experimental/simulation concentration data
- Comparison of scalar gradient distributions
- Visual inspection of velocity fields
- Comparison of velocity-fluctuation distributions
- Spectral comparison of velocity fields

Results: Numerical Validation

experiment **simulation**

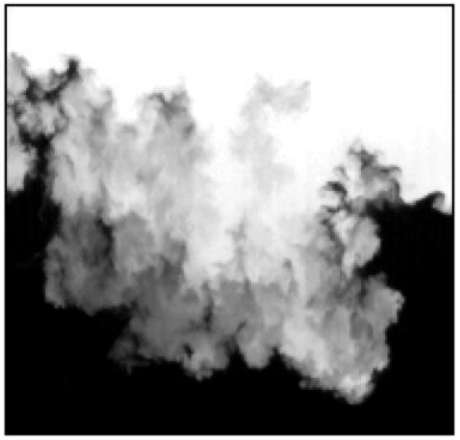

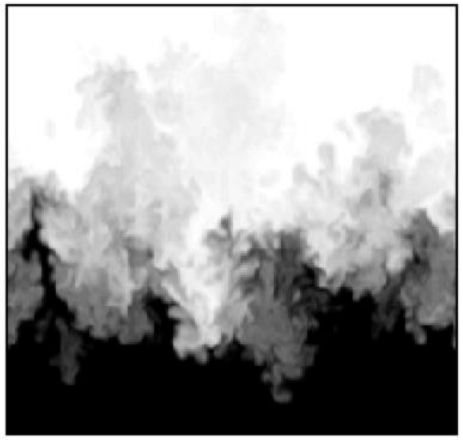

Miranda, *LLNL*
Navier-Stokes Code
10th order-spatial
4th order time
(Cook, PoF, 2007)

Note: Simulation not meant to exactly model experiment

Advection Corrected Correlation Image Velocimetry

Advection equation:

$$\frac{\partial I}{\partial t} = -(\mathbf{v} \cdot \nabla) I$$

(I = pixel intensity)

NEEDS GRADIENTS!

Transverse gradient distribution

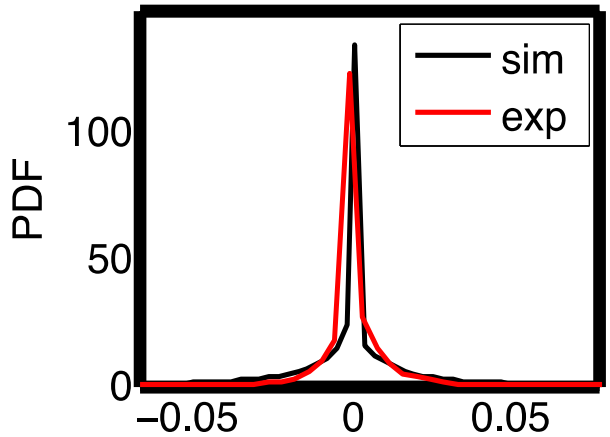

Streamwise gradient distribution

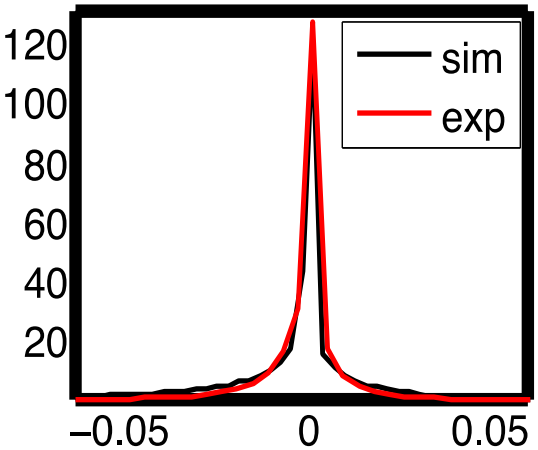

Results: Numerical Validation

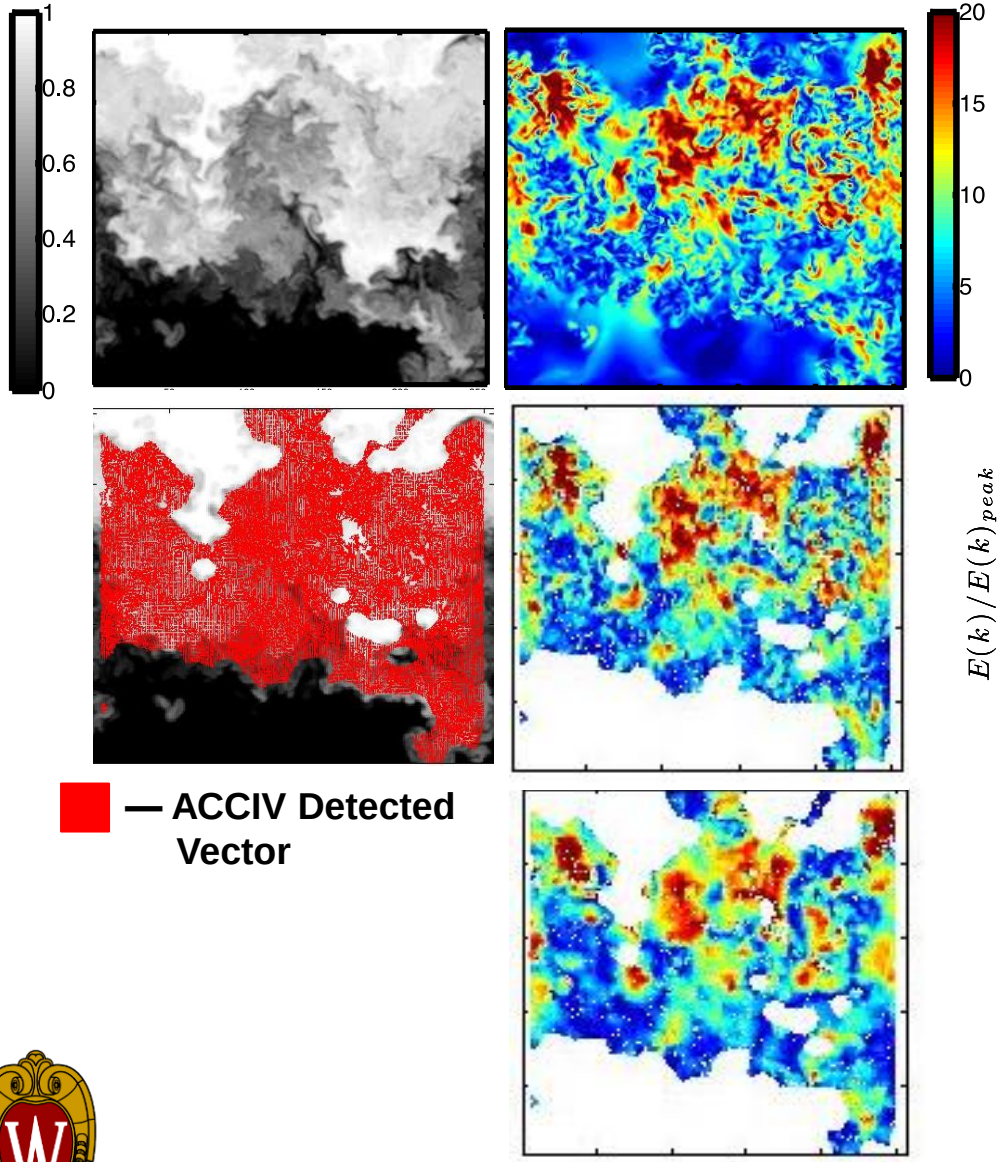

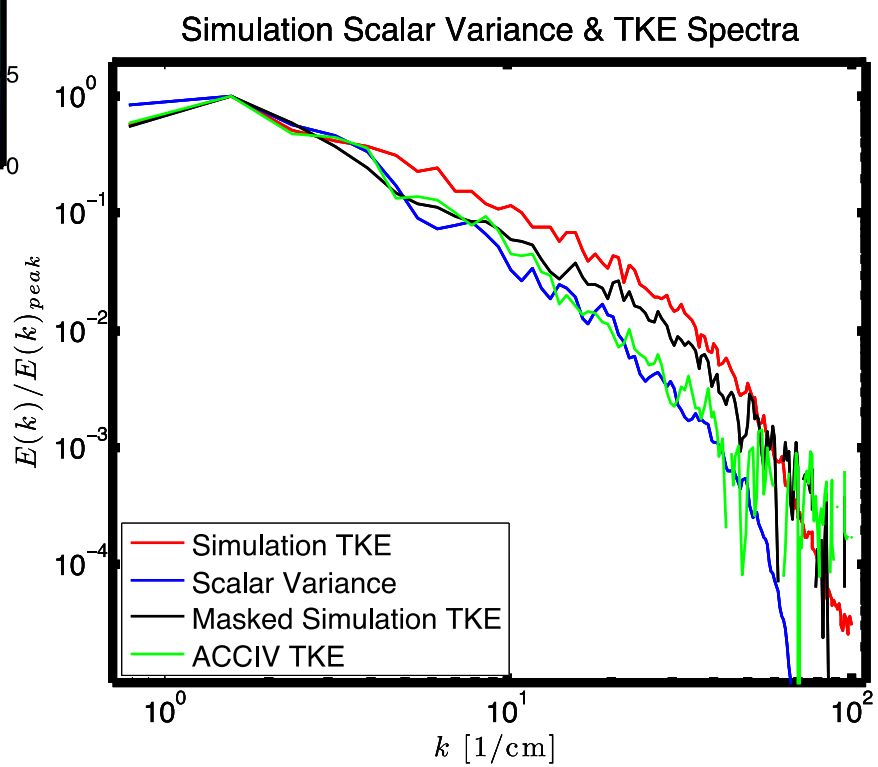

Results: Numerical Validation

ACCIV extracts correct velocity where it is able to detect vectors (within mixing layer)

Transverse Velocity PDF

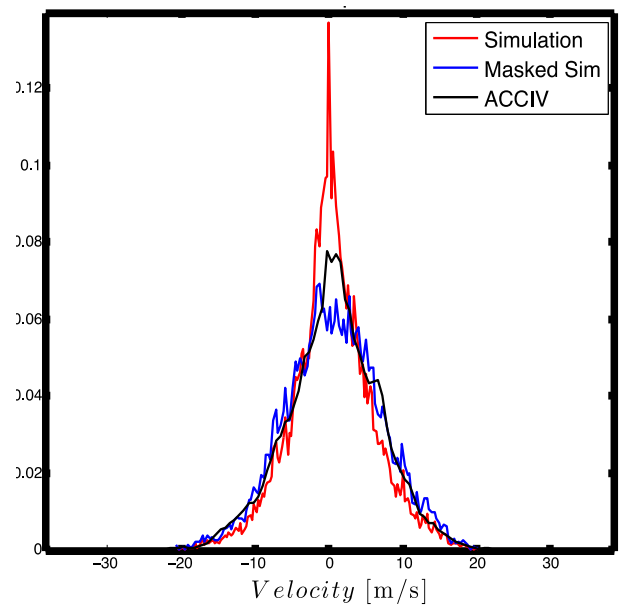

Streamwise Velocity PDF

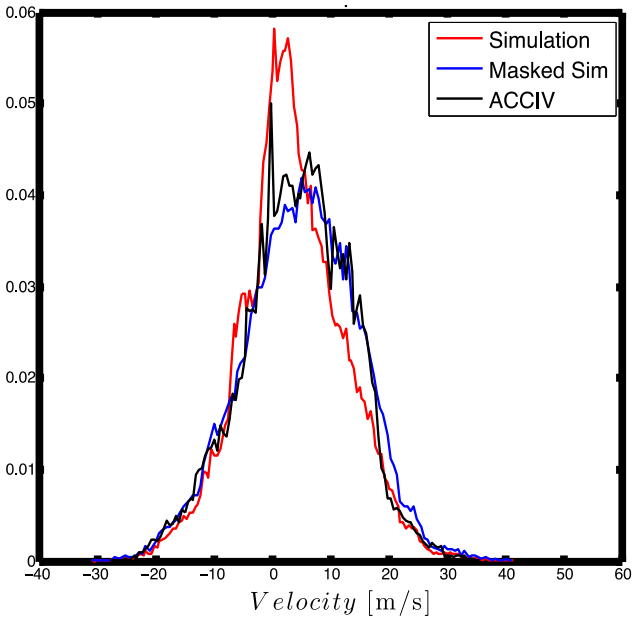

Velocity Magnitude PDF

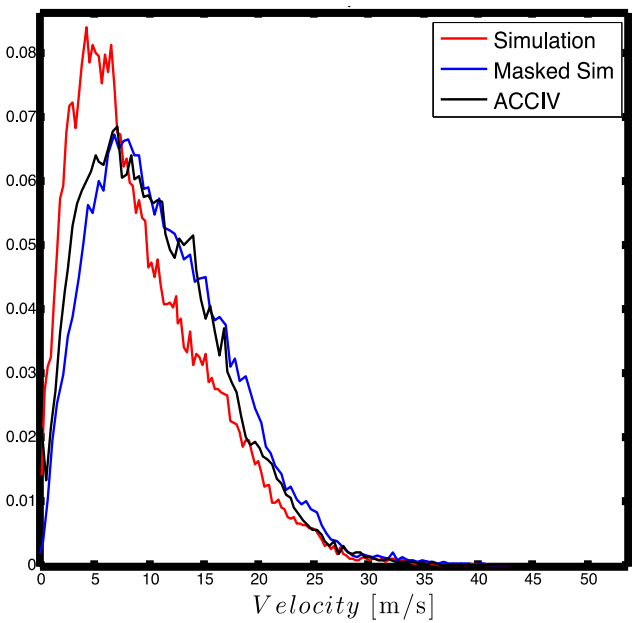

- ACCIV is successfully compared with simulation provided simulation is properly masked

Results: Velocity—Structure

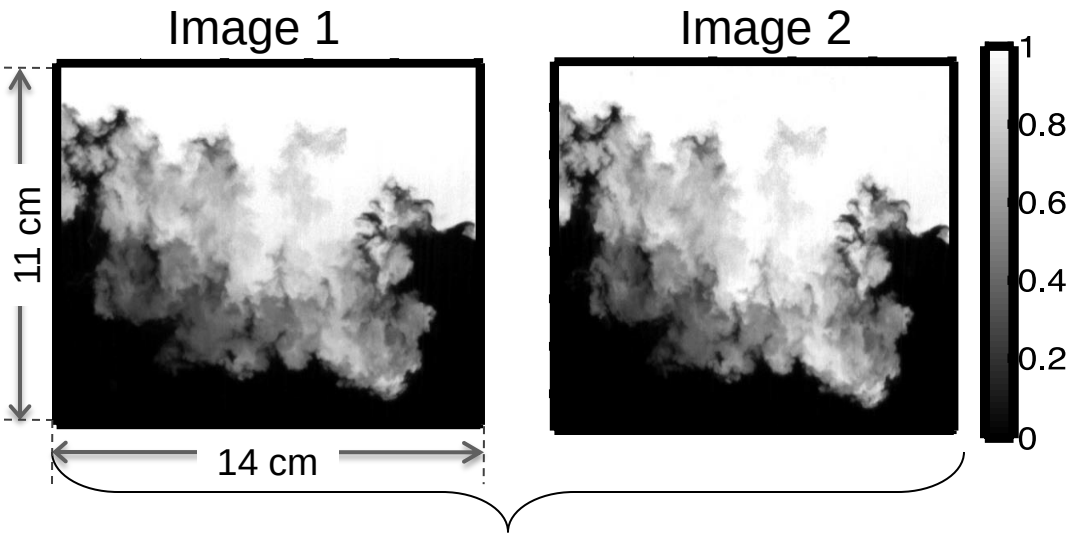

ACCIV

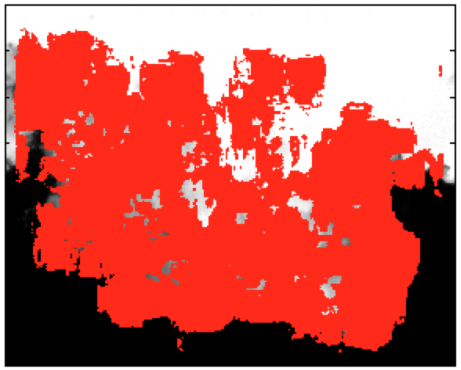

— ACCIV Detected Vector

Note a close correlation of regions without detected vectors to pure (white or black) scalar regions

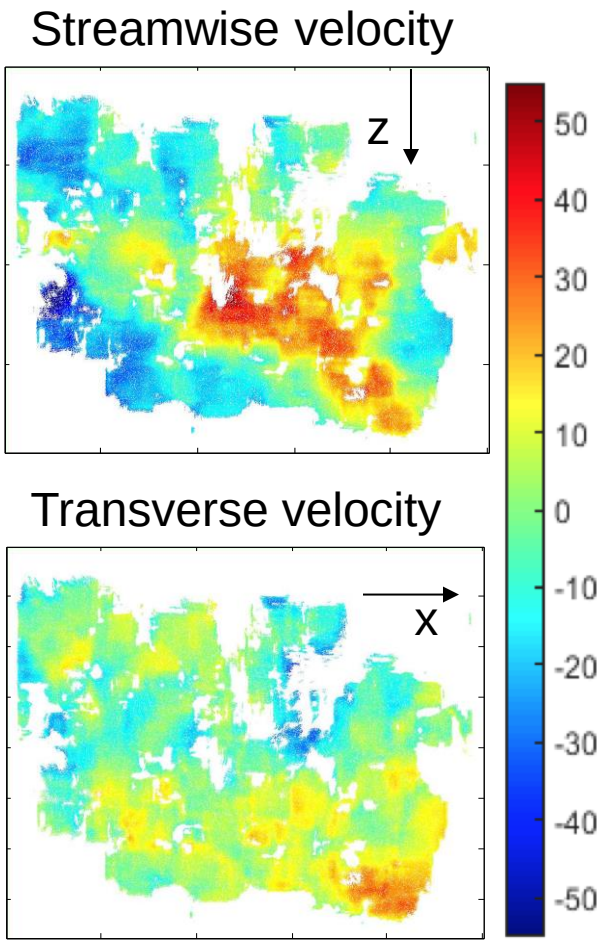

Note: Mean velocity is subtracted from each field to give velocity fluctuations

Results: Velocity—Distribution

- Averaged over 8166 rows from $0.05 < \langle \xi \rangle < 0.95$ region
- Broader distribution of velocities in streamwise direction
- 99% of the velocity lies between:
  - Transverse: ±42.2 m/s
  - Streamwise: ±59.5 m/s

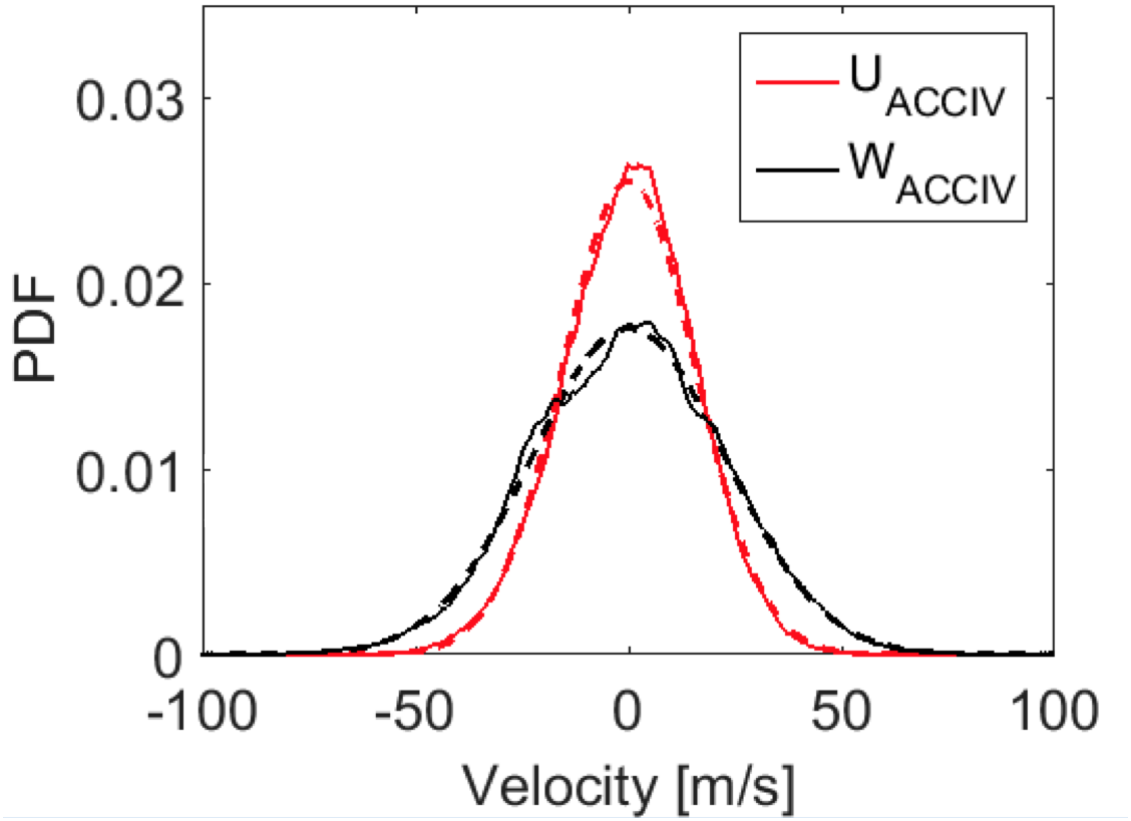

Roughly Gaussian Profiles:
Transverse: σ=15.6 m/s
Streamwise: σ=22.7 m/s

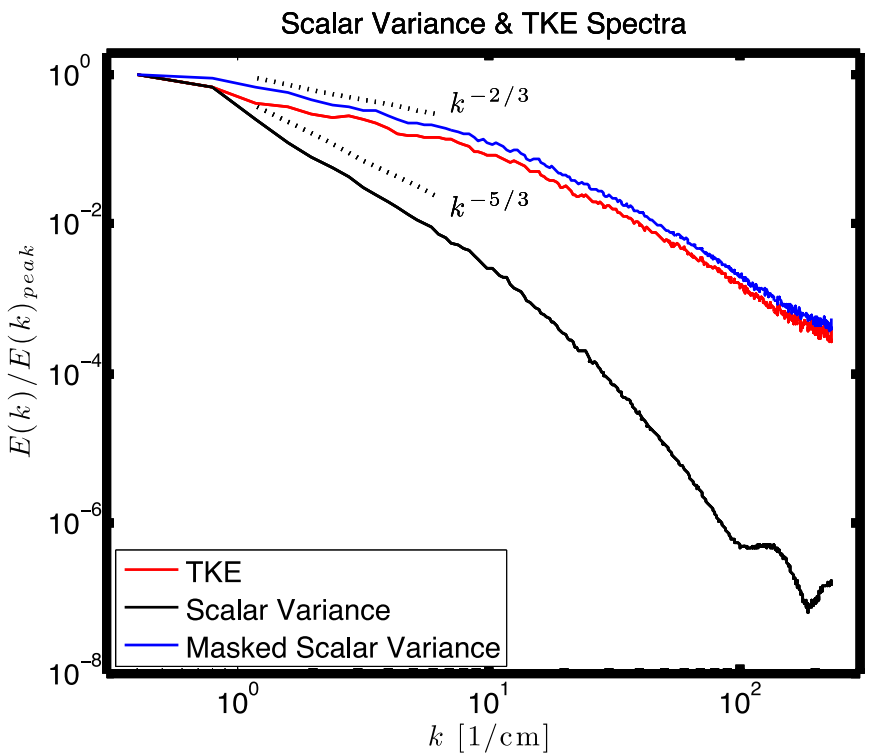

1D Scalar Variance Energy Spectrum

- Averaged over 8168 rows
- From 0.05 < $\langle \xi \rangle$ < 0.95

1D Turbulent Kinetic Energy Spectrum

- Experimental |V| field output from ACCIV
- Same $\langle \xi \rangle$ range & averaging as scalar

Masked 1D Scalar Variance Energy Spectrum

- Masked to keep data only where ACCIV detects vectors

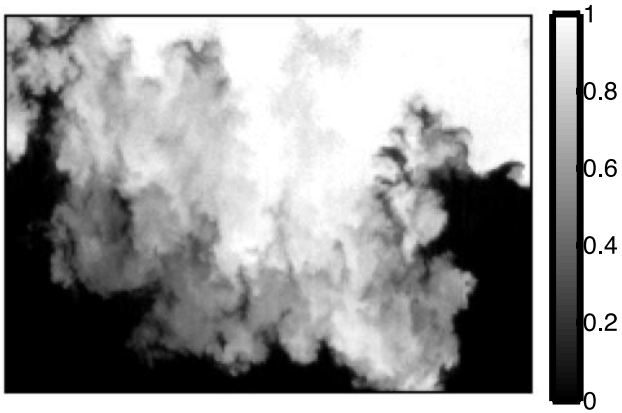

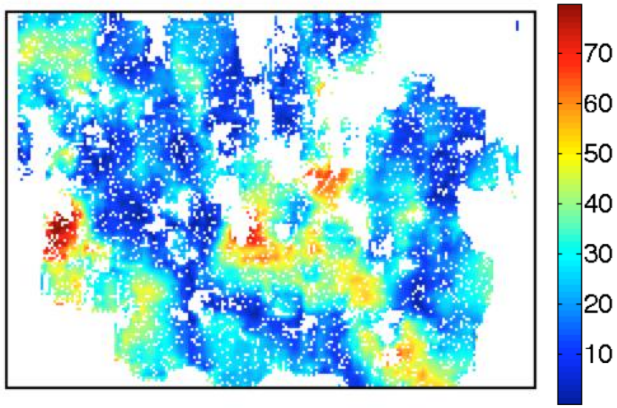

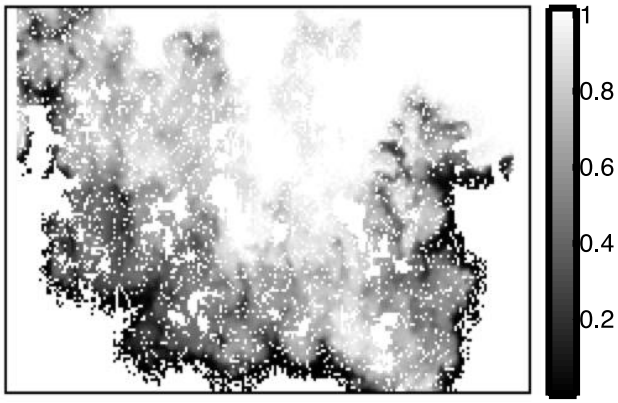

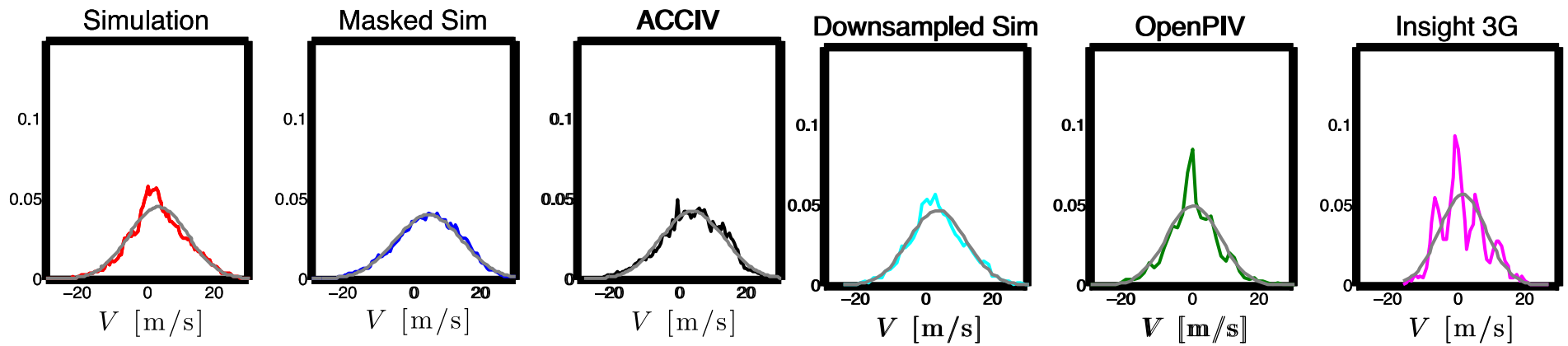

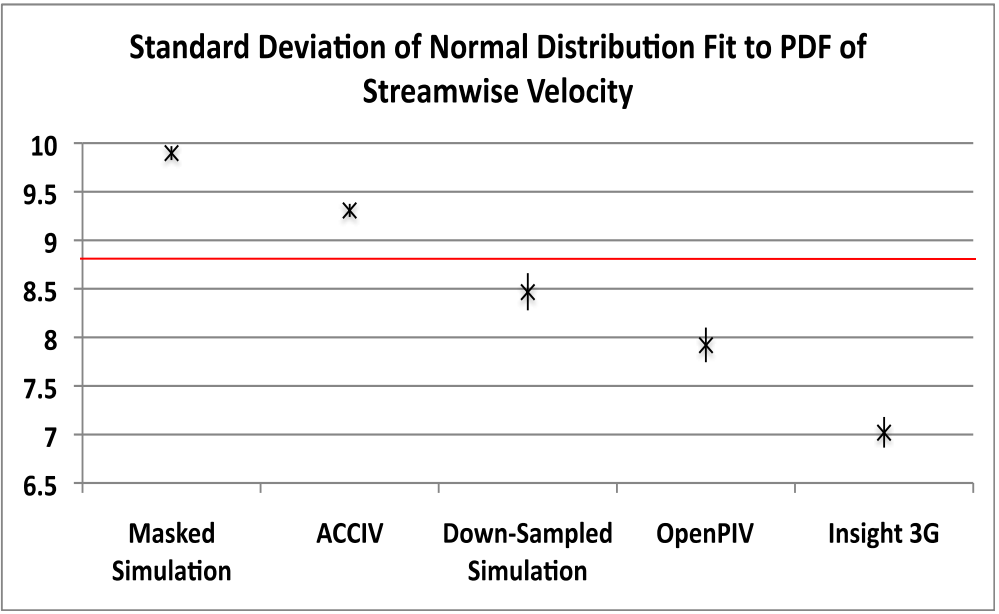

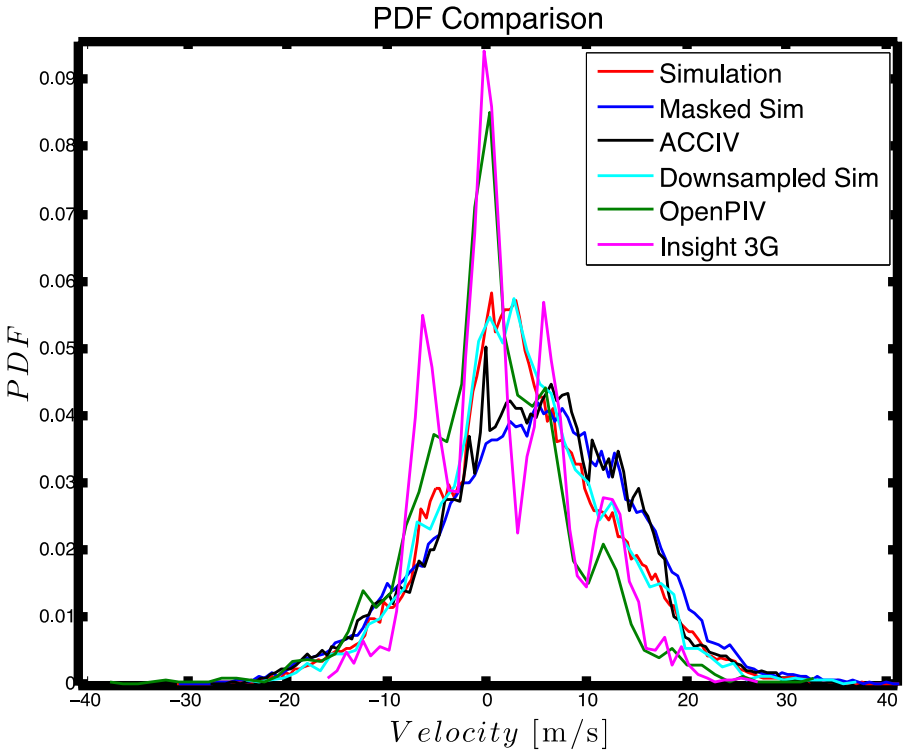

: simulation standard deviation value

Results: Estimate of Reynolds Number

Using previous measurements of the Taylor microscale, λ, made by Weber *et al.* (2012), an estimate of the Taylor Reynolds number (Re_λ) can be found by:

$$Re_{\lambda,i} = \frac{\langle u_i^2 \rangle^{\frac{1}{2}} \lambda}{\nu}$$

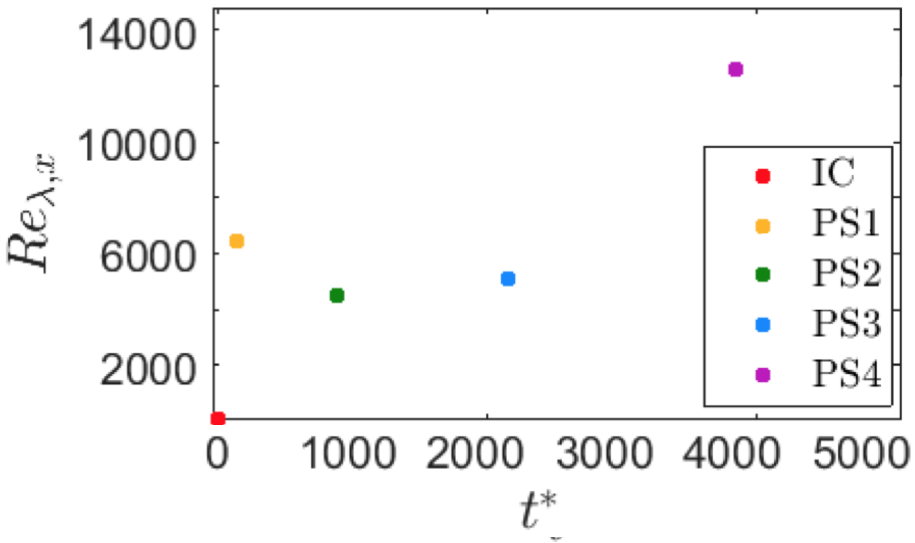

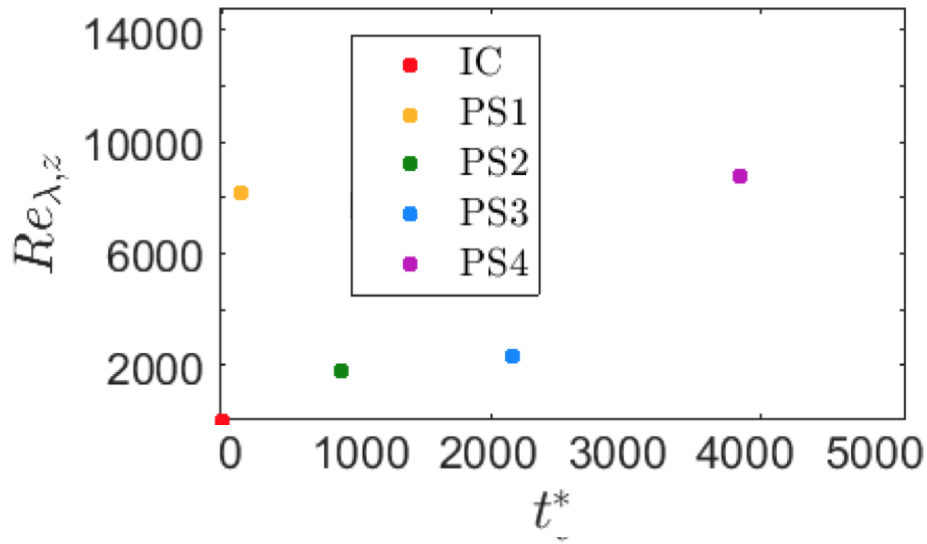

Note: This rising trend in Re_λ is in contrast to results found by others (Lombardini, 2011). This is perhaps due in part because here Re_λ is for the fluctuating velocity components within the mixing layer only.

Results: Insight 4G Settings

PIV Processing Settings

Processor
Recursive rectangular grid – *Multi-pass method with search box refinement*
Direct correlation engine – *Increases the displacement measurement accuracy*

Search box
128→16 with 50% overlap
Chosen to maximize velocity resolution while maintaining confidence in vectors

Spot mask engine
Zero pad mask
Subtracts average intensity from each pixel

Peak engine
Bilinear peak
Fits a set of linear functions to highest intensity pixel and 4 nearest neighbors

Summary & Future Work

Velocity-fluctuation evolution within the mixing layer using PIV

- Broadening, nearly-Gaussian distribution of velocity fluctuations
- Initial rapid increase in Re after passage of shockwave, followed by slight drop, and then gradual increase
- Vorticity shows a peaking, followed by a spreading in distribution
- Post-shock planar TKE spectra flatten in the inertial range when compared to IC spectrum
- The plot of K vs. $-S$ shows decent agreement with theory in x-direction, while z-direction shows higher power law relationship

Future: Simultaneous PIV/PLIF measurements at four post-shock locations

- Second PIV seeder will allow for seeding outside of shear layer as well, filling holes in data
- Allows for concurrent measurement of concentration and velocity, giving better estimate of Taylor Reynolds number, etc.

Questions?

Extra Slides

Background: The Richtmyer-Meshkov Instability

Vorticity Transport Equation:

$$\frac{D\vec{\omega}}{Dt} = (\vec{\omega}\cdot\nabla)\vec{V} - \vec{\omega}\left(\nabla\cdot\vec{V}\right) + \nu\nabla^2\vec{\omega} + \frac{1}{\rho^2}(\nabla\rho\times\nabla p)$$

baroclinic production

Impulsive growth rate:

$$\frac{dh}{dt} = kV_0 A\, h_0 \qquad k = \frac{2p}{l} \qquad A = \frac{r_2 - r_1}{r_2 + r_1}$$

Single Mode Perturbation

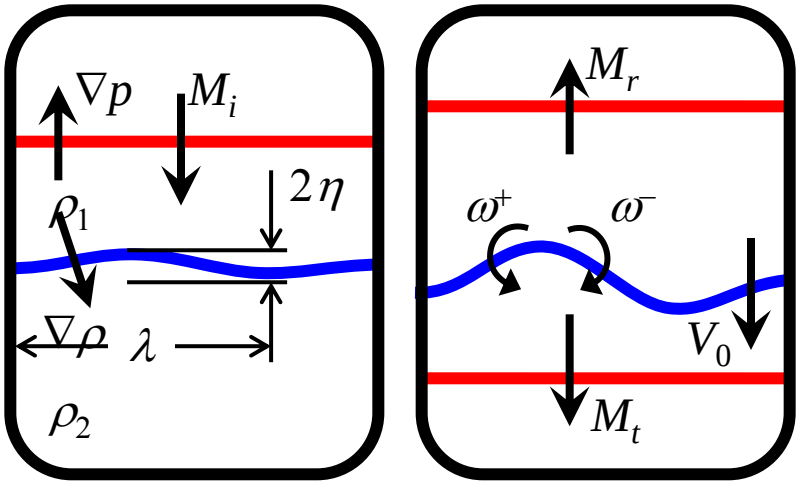

$\rho_2 > \rho_1$

Broadband Perturbation

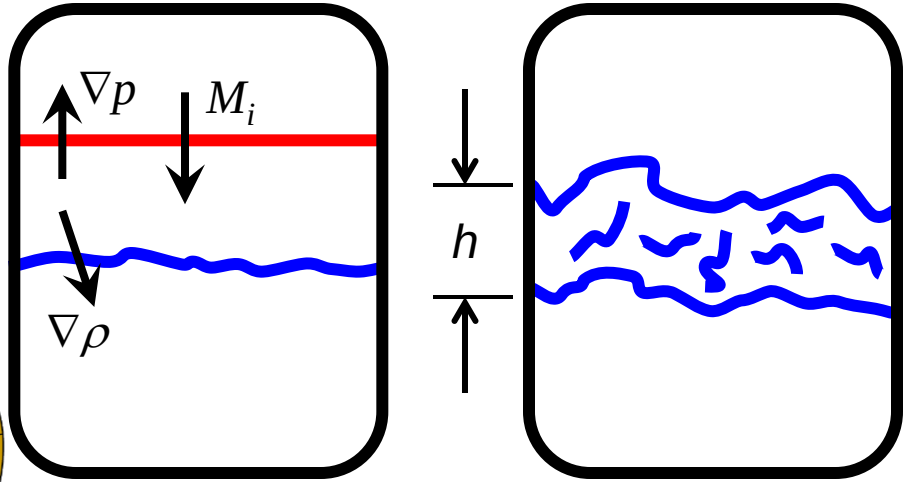

Taking length scale, *h*, velocity scale, *V*

Kinetic energy: $K = \frac{1}{2}\bar{r}hV^2$

Dissipation of kinetic energy: $\frac{dK}{dt} = -cK\frac{V}{h}$

Velocity/kinetic energy relation: $\frac{dh}{dt} = V$

Solution: $h \mu t^q$

Background: Motivation

RMI plays out over a large range of length and time scales, and has application in many fields of science & engineering [e.g. Astronomy, aerospace, inertial confinement fusion (ICF)]

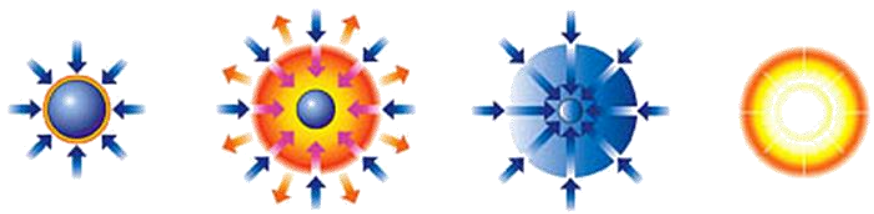

Radiative heating | Ablation | Compression | Thermo-nuclear burn

	ICF	Shock tube
L scale	10^{-6} m	10^{-2} m
t scale	10^{-9} s	10^{-6} s
ρ scale	10^{3} kg/m^3	10^{0} kg/m^3
M	~30	≤ 5
A	[-1,1]	[-1,1]

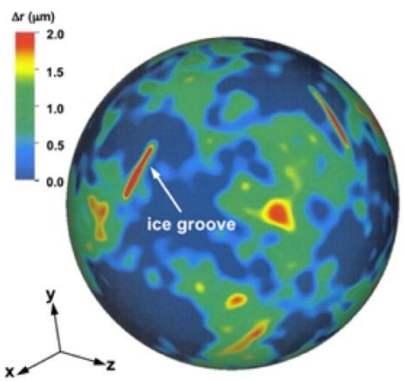

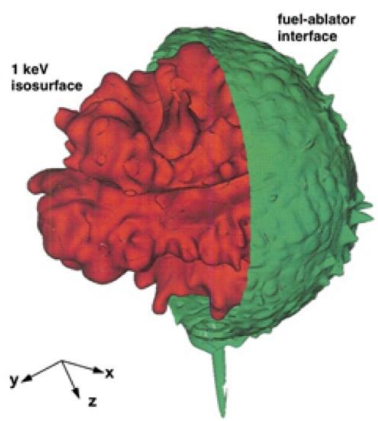

Goal: Better understand shock-induced turbulent mixing in ICF by performing hydrodynamic experiments in a shock tube

Background: Evolution of RMI Studies

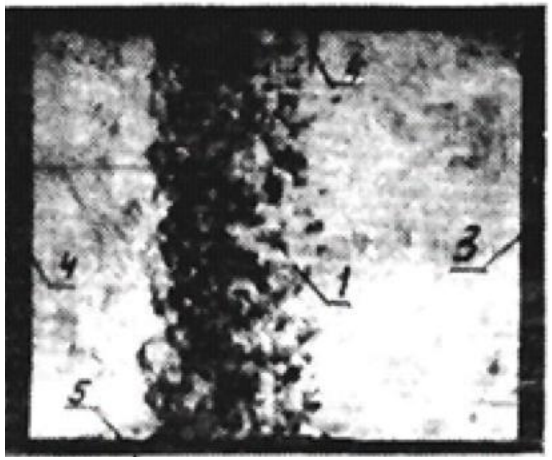

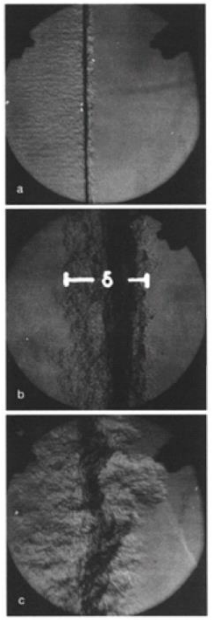

Early Work

- Horizontal shock tubes
- Utilized membranes
- Integrated measurements
  - Schlieren
  - Shadowgraph
- Limited to measurement of large-scale statistics
  - Amplitude/thickness

Later Work

- Vertical shock tubes introduced
- Membraneless interfaces
- Planar measurements
  - PLIF
  - PIV
- Ability to measure fields
  - Concentration
  - Velocity

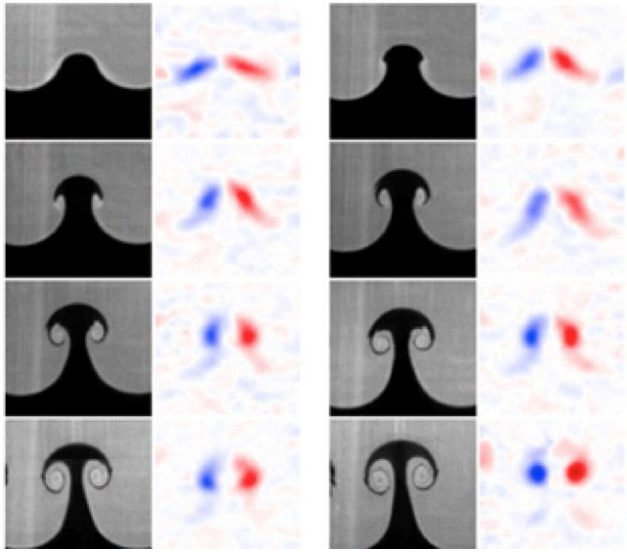

Background: Relevant Studies

University of Arizona

- Vertical
- Membraneless
- Single Mode

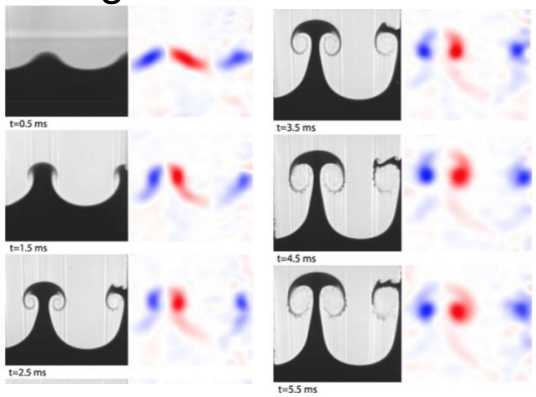

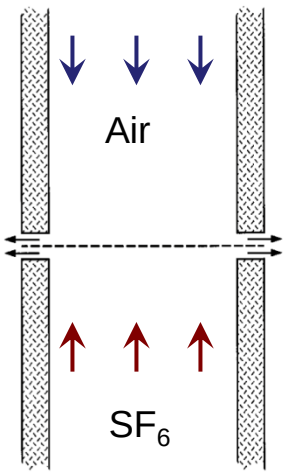

Los Alamos National Lab (LANL)

- Horizontal
- Gas curtain
- 2-interface

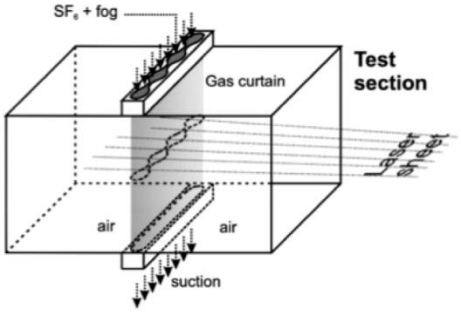

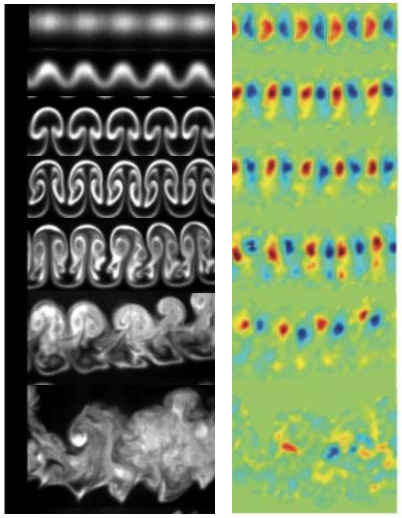

Texas A&M University (Now GA Tech)

- Inclined interface ($0° < \theta < 90°$)
- Membraneless
- Shock & reshock

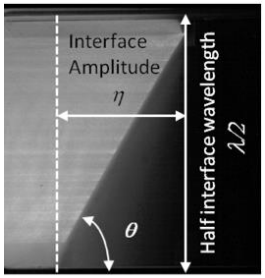

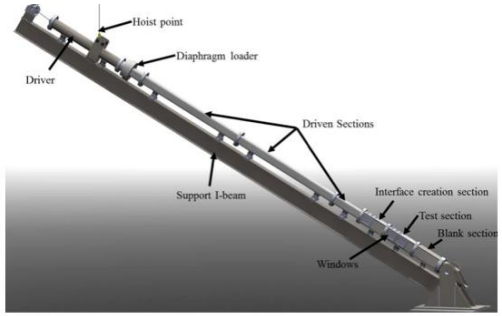

University of Wisconsin

- Acetone PLIF → Concentration
- Multimode, shear layer initial condition
- Evolution of mixing layer structure

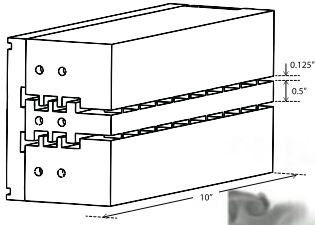

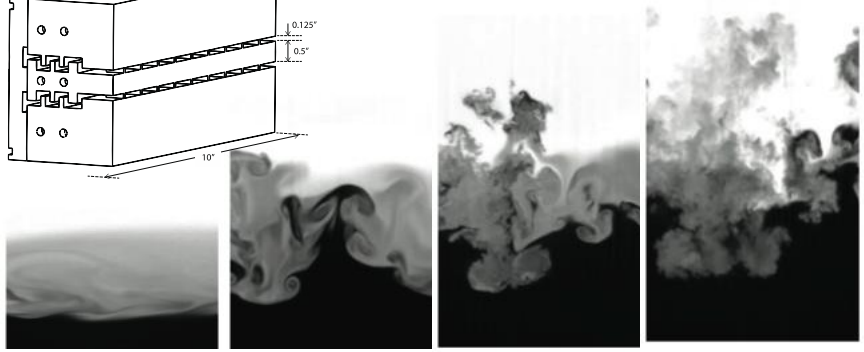

Background: Pulsed Light Velocimetry

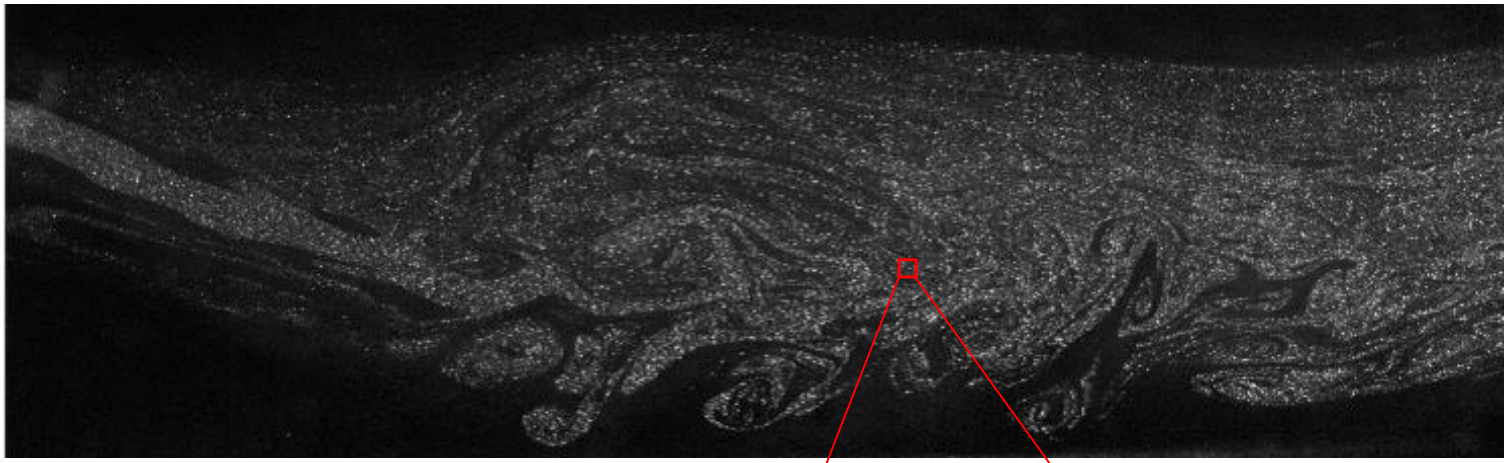

Particle displacement, Δx, determined by particle image velocimetry (PIV) or correlation image velocimetry (CIV) algorithm. With a known inter-frame time, Δt, velocity given by

$$\boldsymbol{u}(\boldsymbol{x}, t) = \frac{\Delta \boldsymbol{x}(\boldsymbol{x}, t)}{\Delta t}$$

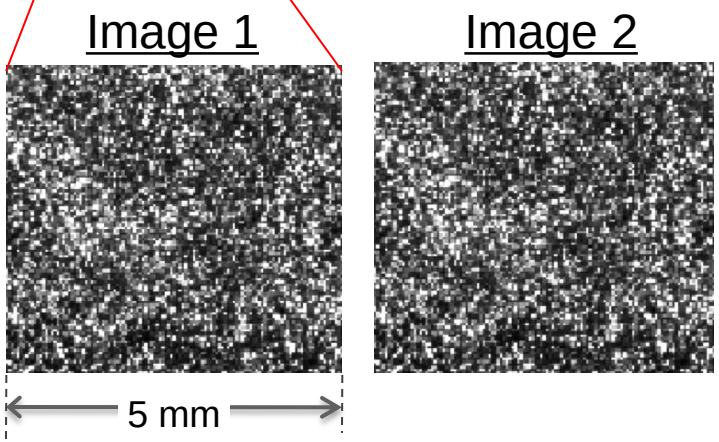

Shown here is PIV method; however, the concept is the same for CIV, where pattern-matching is used (rather than particles) to mark portions of the flow.

Slots Section

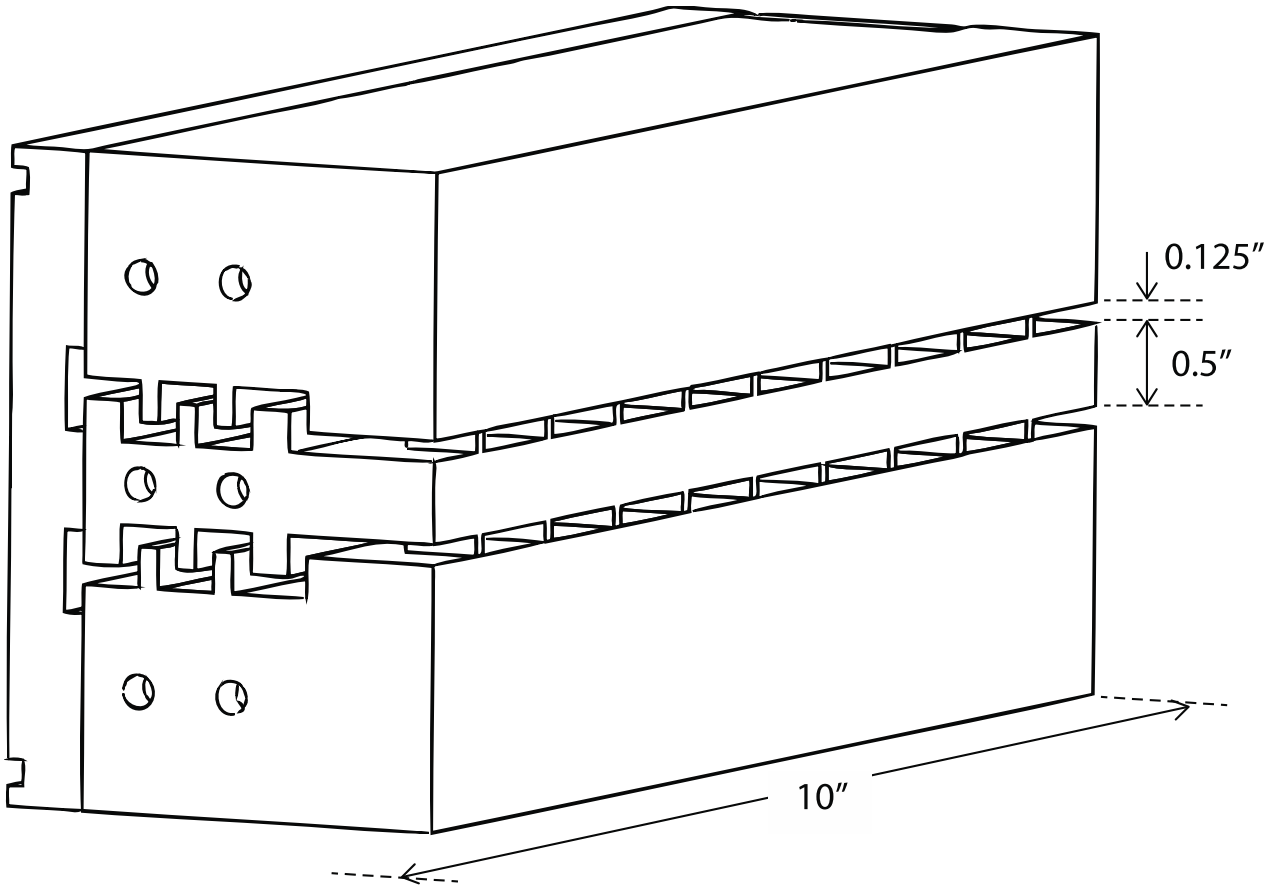

Results: Higher-order statistics

Normalized velocity-derivative moments:

$$M_n = \left\langle \left(\frac{\partial u_1}{\partial x_1} \right)^n \right\rangle \Big/ \left\langle \left(\frac{\partial u_1}{\partial x_1} \right)^2 \right\rangle^{n/2}$$

For n=3 & n=4, these are the velocity-derivative skewness (*S*) and kurtosis (*K*), respectively.

Theory states, and experiments have shown (Van Atta and Antonia, 1980) that $K \sim Re^{3/8}$.

Additionally, theory and experiments imply a relationship between *K* and *S* as $-S \sim K^{3/8}$.

Results: Higher-order statistics – Skewness

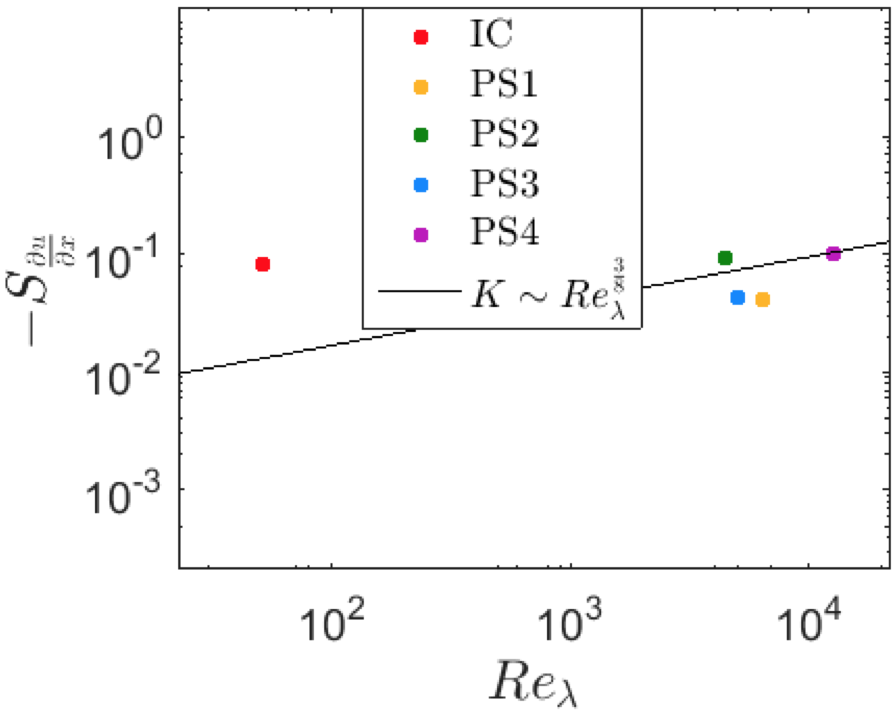

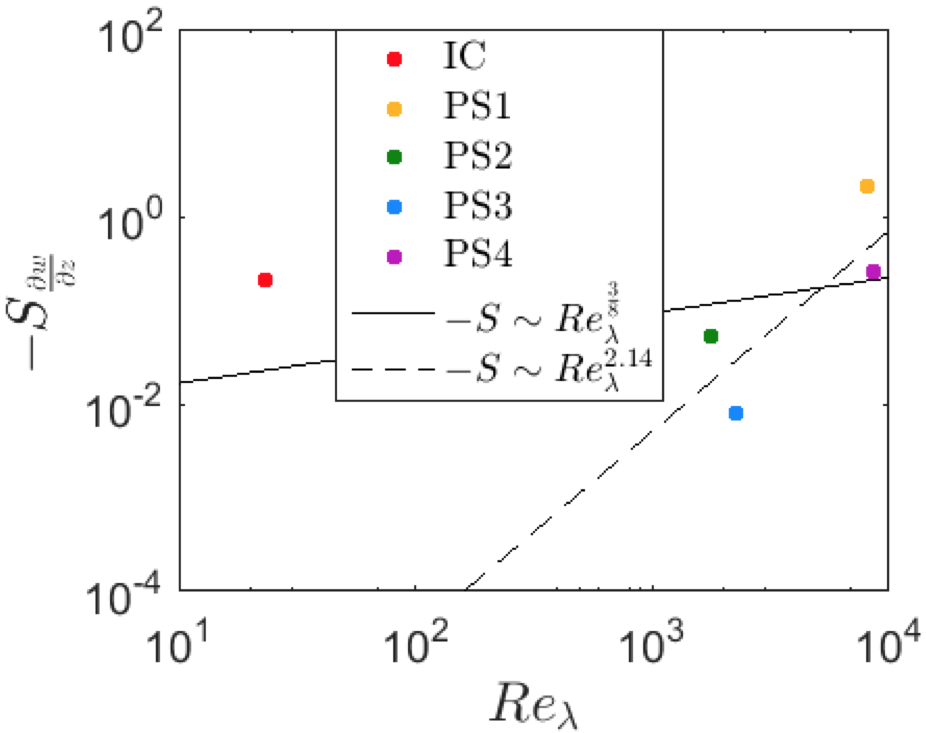

Velocity-derivative Skewness

$$S_{\frac{\partial u_i}{\partial x_i}} = \left[\frac{\left\langle \left(\frac{\partial u_i}{\partial x_i} \right)^3 \right\rangle}{\left\langle \left(\frac{\partial u_i}{\partial x_i} \right)^2 \right\rangle^{1.5}} \right]$$

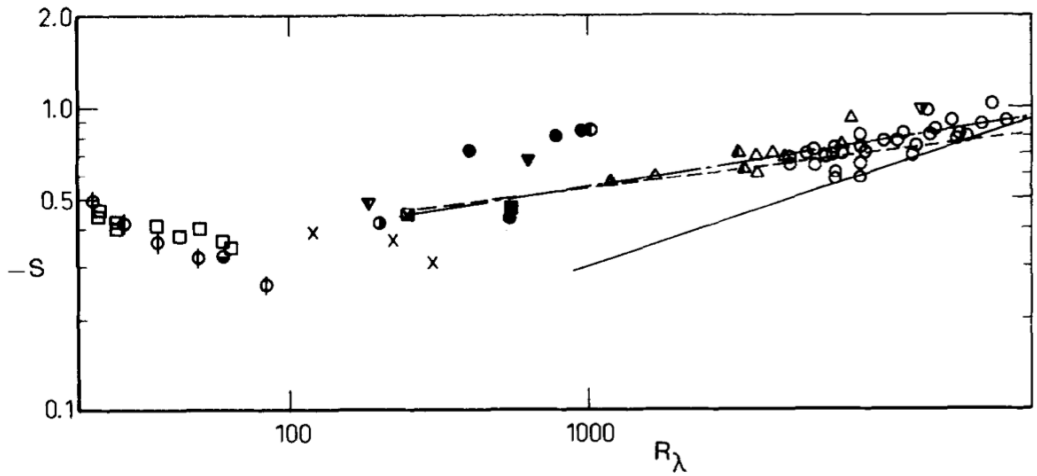

Results: Higher-order statistics – Kurtosis

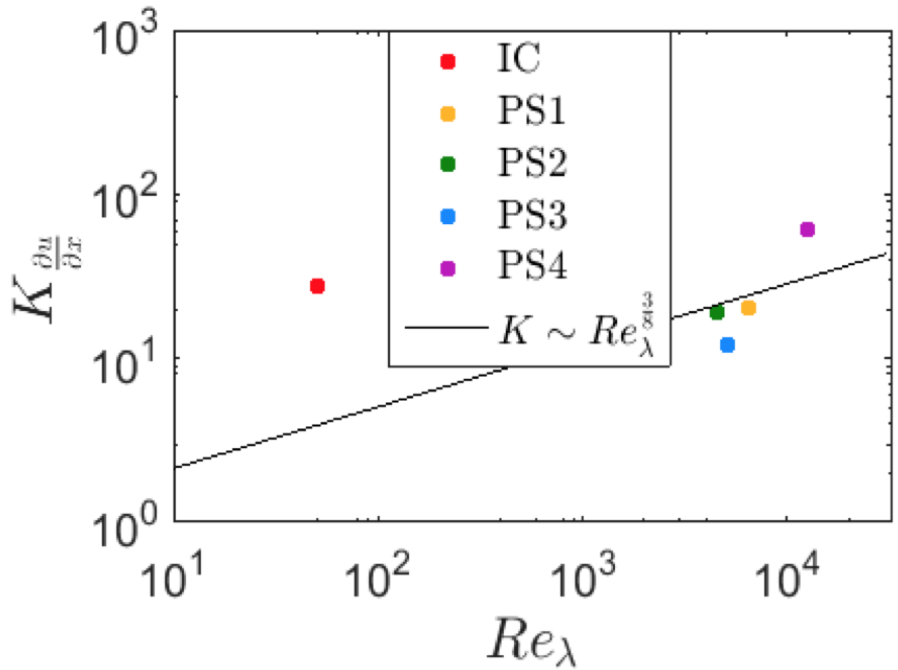

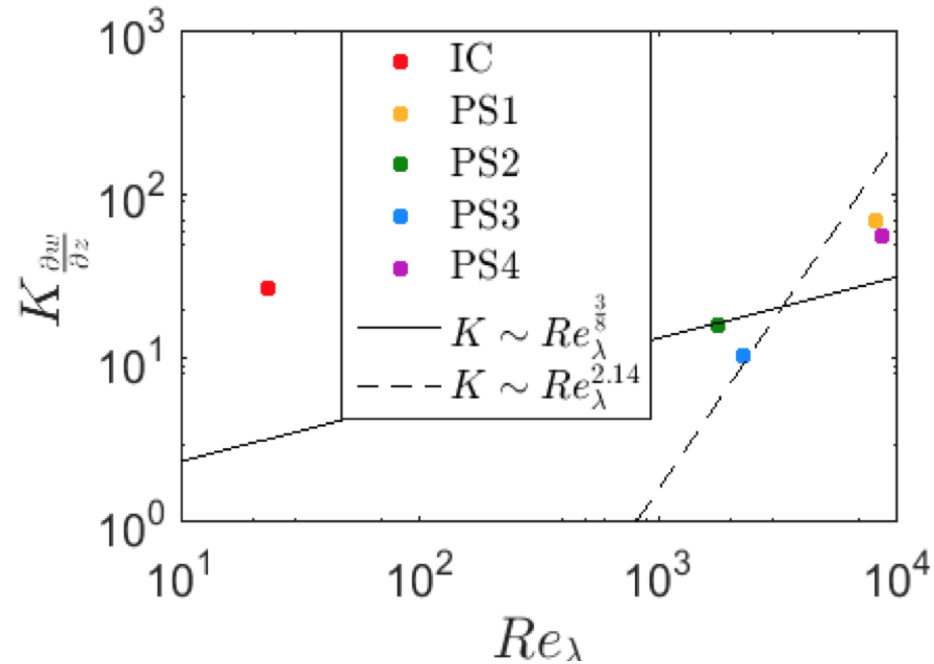

Velocity-derivative Kurtosis

$$K_{\frac{\partial u_i}{\partial x_i}} = \left[\frac{\left\langle \left(\frac{\partial u_i}{\partial x_i} \right)^4 \right\rangle}{\left\langle \left(\frac{\partial u_i}{\partial x_i} \right)^2 \right\rangle^2} \right]$$

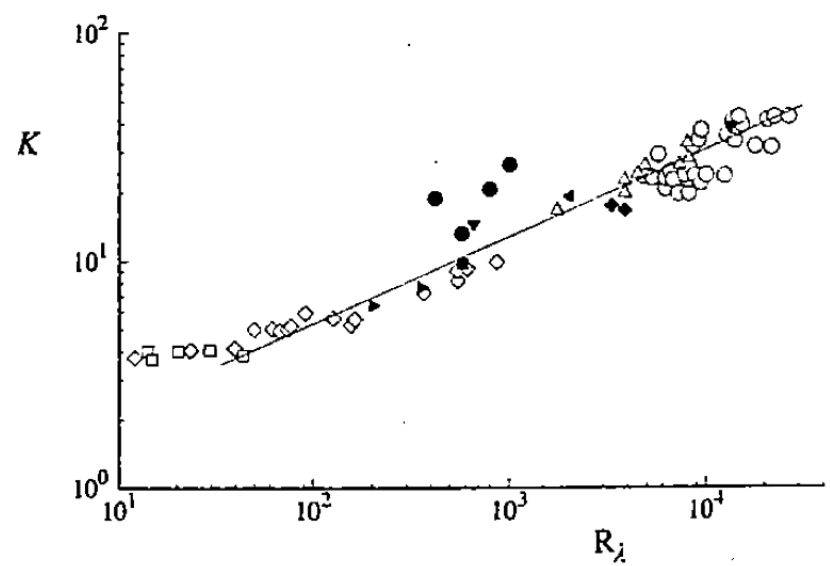

Results: Higher-order statistics – S vs. K

Historically, results have shown $-S \sim K^{0.362}$ (Van Atta)

While a similar trend is seen in *x*-direction, we notice a steeper power law relationship in *z*-direction

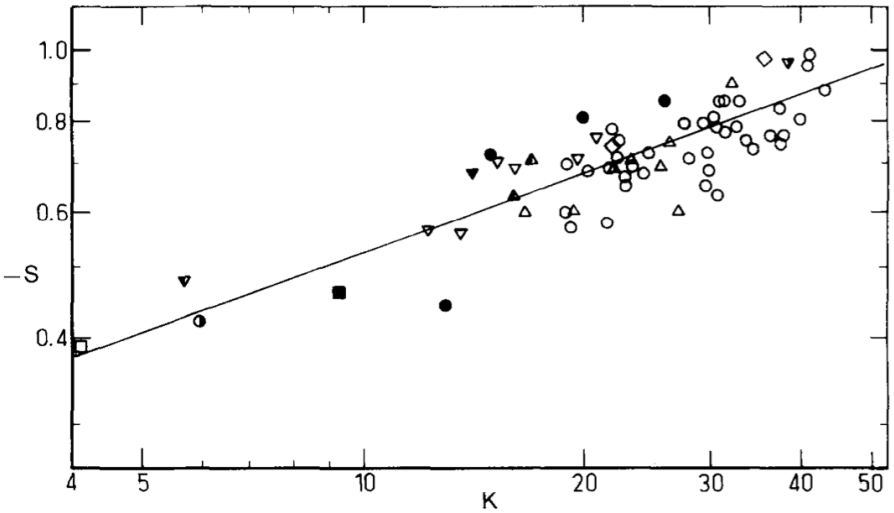

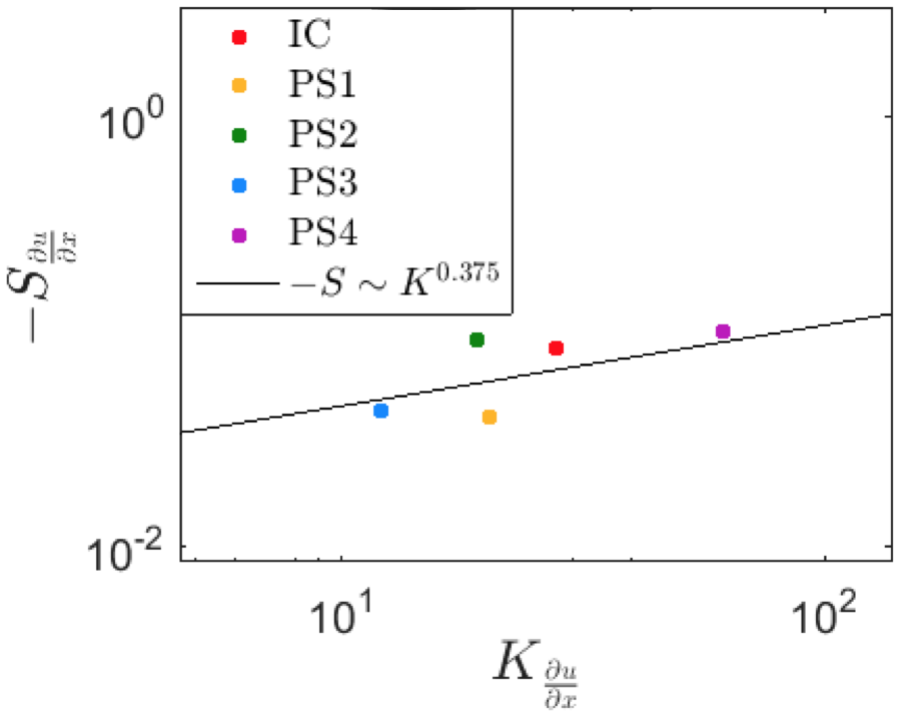

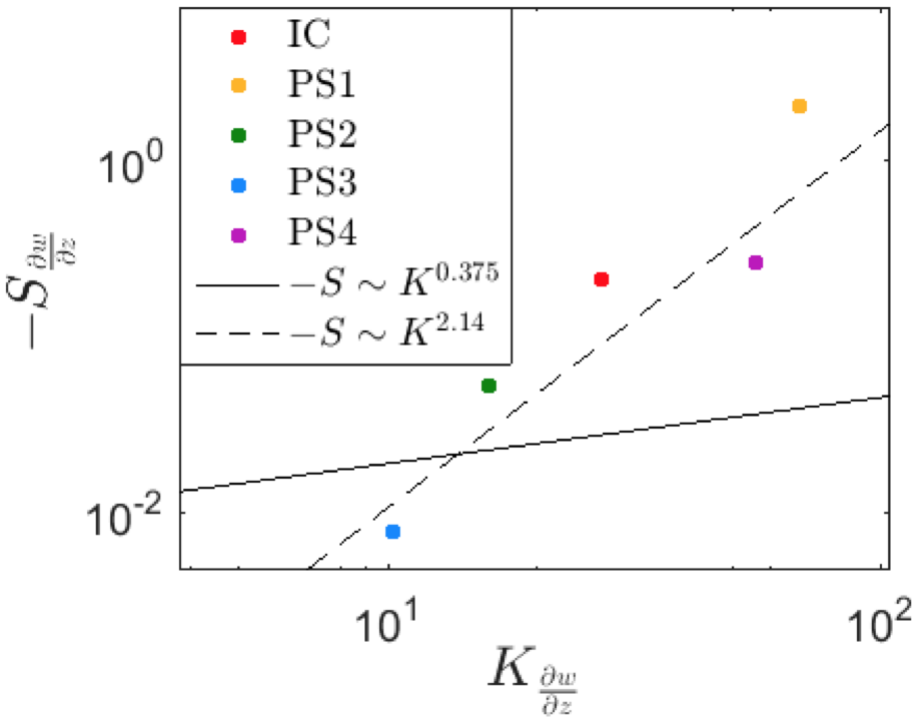

Results: Spectra

Scalar Variance Energy Spectra (within $0.1 < \langle \xi \rangle < 0.5$)

- Slope at low k decreases in time
- Inertial range at two latest times, 1.5 $cm^{-1} < k < 7$ cm^{-1}
- $k^{-5/3}$ inertial range slope, not $k^{-3/2}$ (Zhou, POF, 2001)

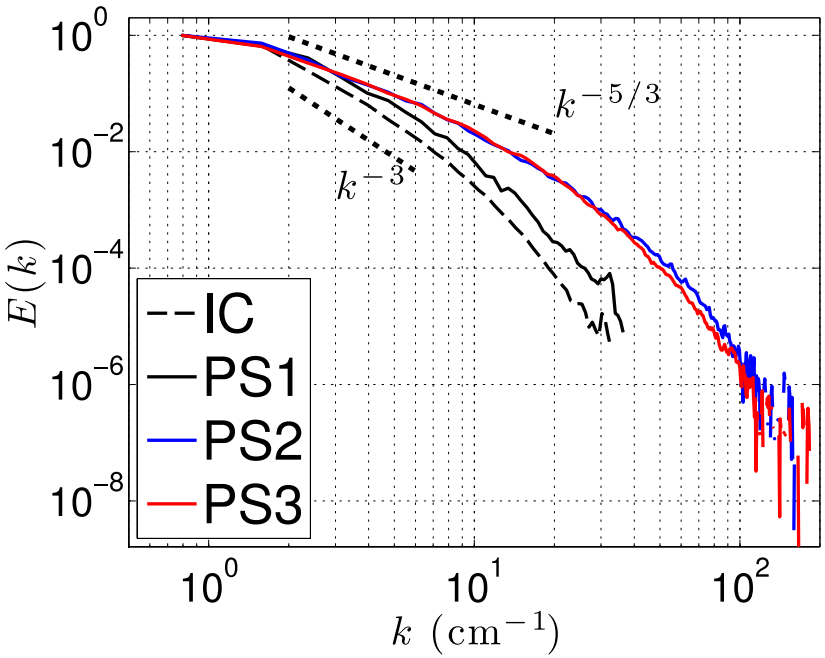

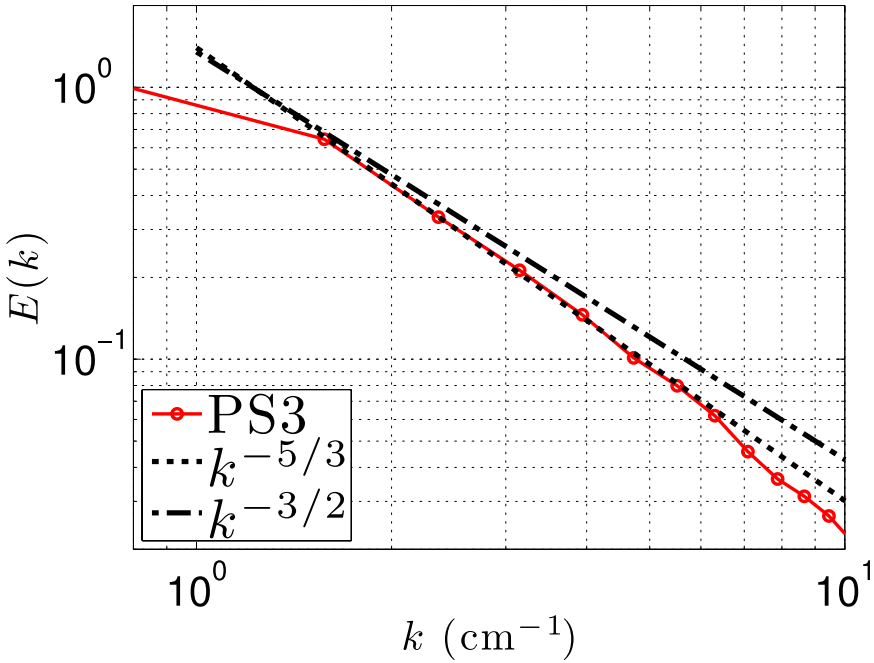

Summary & Conclusions

M=2.2 (PLIF) CIV Experiments

- Spectra show a $k^{-5/3}$ inertial range for scalar data
- Masking effects lead to a $k^{-2/3}$ inertial range for velocity data
  (This is not physical, real slope is steeper)
- ACCIV returns correct values where it is able to detect vectors
  - Detects a large number of velocity vectors
  - Potentially higher resolution than PIV results
  - Main drawback is “patchiness” of located vectors in experimental data

M=1.4 PIV Experiments

- Broadening, nearly-Gaussian distribution of velocity fluctuations
- Vorticity shows a peaking, followed by a spreading in distribution
- Post-shock planar TKE spectra flatten in the inertial range when compared to IC spectrum
- The plot of *K* vs. -*S* shows decent agreement with theory in *x*-direction, while *z*-direction shows higher power law relationship

Background: The Richtmyer-Meshkov Instability

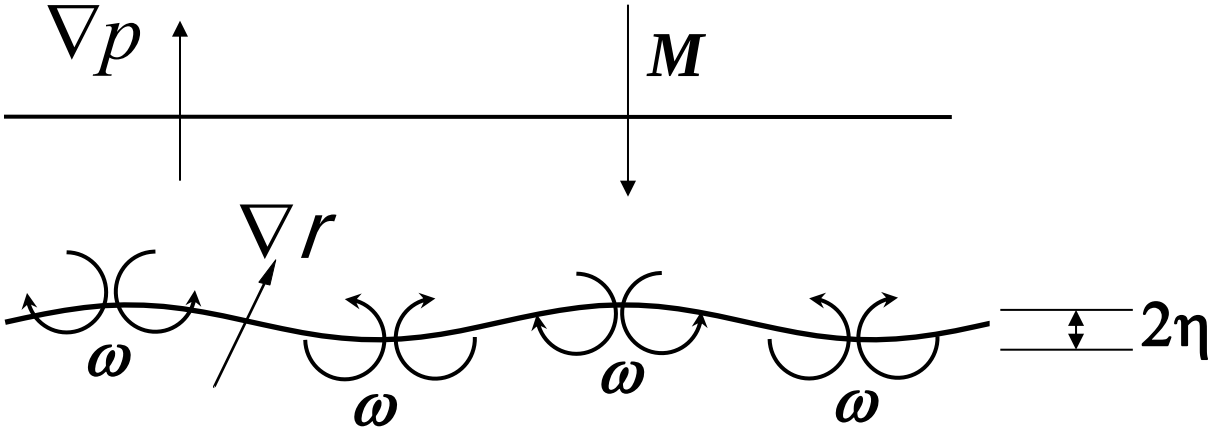

Baroclinic vorticity generation:

$$\frac{dW}{dt} = \frac{\nabla r \times \nabla p}{r^2}$$

Impulsive (linear) model: R. Richtmyer, 1960

$$h = k[V]Ah_0 t$$

- k: wavenumber
- $[V]$: velocity jump
- $A = \frac{\rho_1 - \rho_2}{\rho_1 + \rho_2}$

Valid for $\eta << \lambda$

First experiments: E. Meshkov, 1969